

Supplemental Methods

Cell culture

RPMI8226 and MM.1S human MM, HMEC-1, HS-5, and 293T cell lines were purchased from the American Tissue Type Culture Collection (Manassas, VA, USA). MM cell lines were cultured at 37°C/5% CO₂ in RPMI-1640 media (Gibco, Rockville, MD, USA) containing 10% fetal bovine serum, 2% GlutaMAX (Gibco, Rockville, MD, USA), 100 U/mL penicillin, and 100 µg/mL streptomycin. HMEC-1 was cultured in MCDB131 media (Gibco, Rockville, MD, USA) containing 10% fetal bovine serum, 2% GlutaMAX, 10 ng/mL epidermal growth factor (EGF), 1 µg/mL hydrocortisone, 100 U/mL penicillin, and 100 µg/mL streptomycin. HS-5 and 293T were cultured in DMEM (Corning, Tewksbury, MA, USA) containing 10% fetal bovine serum, 100 U/mL penicillin, and 100 µg/mL streptomycin. All the cell lines were mycoplasma negative and authenticated by short tandem repeat (STR) genotyping.

Purification of maltose-binding protein (MBP)-tagged proteins

Purification of MBP-PTR1 and MBP proteins was done as described in De Bakshi et al¹. Briefly, the cDNA sequence encoding the HAPLN1-PTR1 domain (aa 159-253) was inserted into pET28-MBP-TEV plasmid in frame with and downstream of the MBP coding sequence and the resulting plasmid was transformed into the BL21 Rosetta 2 *Escherichia coli* strain. Proteins were induced with 1 mM IPTG followed by purification using amylose resin and elution by 50 mM maltose. To remove potential LPS contamination, the eluted protein fraction was run through Pierce High-Capacity Endotoxin Removal Spin Columns (Thermo Scientific, Waltham, MA, USA) according to the manufacturer's instruction. The

LPS-removed protein fraction was further processed by fast protein liquid chromatography (FPLC) using a size exclusion column, Superose 6 Increase 10/300 GL (Sigma-Aldrich, St. Louis, MO, USA) to obtain highly purified, monomeric and functional recombinant HAPLN1-PTR1 domain. The purity of the protein fragment was assessed by SDS-PAGE analysis and Coomassie staining and the functional activity was ensured by assessing NF- κ B activation in MM cell lines via electrophoretic mobility shift assay (EMSA) as described previously². Cells were treated with either 100 nM MBP-PTR1 or MBP alone, unless indicated otherwise.

Adhesion assay

The glass plates (6 mm diameter well) coated with fibronectin (FN, 10 μ g/mL) or plated with a confluent monolayer of cells (HMEC-1, HS-5) were prepared one day before assaying for MM cell adhesion. Fibronectin-coated plates were blocked with 1% BSA/PBS for 1 hour. MM cells were pre-stained with CFSE (Thermo Scientific, Waltham, MA, USA) according to the manufacturer's instruction and plated on the glass plate (50,000 cells/well in 1% BSA RPMI1640 media) and incubated for 2 hours at 37°C. After incubation, non-adherent MM cells were washed with PBS twice and fixed with 4% paraformaldehyde. The plates were imaged, and cell number was counted by ImageJ software.

Transwell migration assay

The bottom chambers of Transwell filter chambers (5 μ m pores; Corning, Tewksbury, MA, USA) were coated with 10 μ g/ml of FN as described previously³. Cells (5×10^5 and $1 \times$

10^5 for RPMI8226 and MM.1S, respectively) were pre-stained with CFSE (Thermo Scientific, Waltham, MA, USA) according to the manufacturer's instruction and placed in the upper chamber in 1% BSA RPMI1640 media and incubated for 16 hours at 37 °C. In the bottom chamber, chemoattractants were added in 1% BSA RPMI1640 media. Cells on the bottom of the filter were fixed, and four fields were imaged, and the cell number was counted by ImageJ software. For the co-culture of HS-5 and MM cells, HS-5 cells (5×10^4 cells/24-well) were plated in the bottom chamber one day before the migration assay. The media was changed with 1% BSA RPMI1640 media and the Transwell inserts were assembled for the assay.

μ -Slide time-lapse migration assay

The time-lapse migration assays were performed with μ -Slide Chemotaxis (Ibidi GmbH, Planegg, Germany) following the manufacturer's instruction. Briefly, RPMI8226 cells were plated in the complete media in the channel. In the reservoir, the final concentration of 30 nM of MBP or MBP-PTR1 was filled. Images were taken every 10 minutes for 16 hours using a Nikon Eclipse Ti Inverted Microscope (Nikon, Tokyo, Japan) equipped with a CO₂- and temperature-controlled chamber. Images were imported as stacks to ImageJ software and analyzed with the ImageJ plugins, Manual Tracking, and the Chemotaxis and Migration Tools. Individual cells moving at least one cell length were tracked at each cell position in the field throughout the temporal stacks, until the cell could no longer be tracked, e.g., moving out of frame. Calculations of the forward migration index parallel (FMI^{II}) or perpendicular (FMI^I) to the chemotactic gradient were as following^{4,5}.

$$FMI^{II} = \frac{1}{n} \sum_{i=1}^n \frac{y_{i,end}}{d_{i,accum}}$$

$$FMI^+ = \frac{1}{n} \sum_{i=1}^n \frac{x_{i,end}}{d_{i,accum}}$$

(i = index of single cells, n = number of cells, $x_{i,end}$, $y_{i,end}$ = coordinates of the cells' endpoints, $d_{i,accum}$ = accumulated distance of the cells' paths)

Generation of stable HS-5 cells secreting HAPLN1 matrikine

The cDNA sequence encoding the HAPLN1 fragment (aa 32-354) was inserted into the pSecTag2A (Invitrogen, San Diego, CA, USA) plasmid in frame with the N-terminal Igκ chain leader sequence for protein secretion and the C-terminal *c-Myc* epitope and 6×His tag. The integrity of the resulting construct was sequence verified. HS-5 cells were transfected with pSecTag2A empty vector (EV) or pSecTag2A-HAPLN1-32-354 by Nucleofector kit (Lonza, Walkersville, MD, USA). The cells were treated with 100 µg/mL Zeocin (Thermo Scientific, Waltham, MA, USA) and the stable clones (HS-5/EV and HS-5/H1) were selected by limited dilution and clonal expansion. HAPLN1 knockdown cells were generated by shHAPLN1 (SHCLNG-NM_001884, Sigma-Aldrich, St. Louis, MO, USA) transduction and selected with puromycin.

Western blot (WB) analysis of conditioned media (CM) and cell extracts

CM was prepared by culturing a confluent monolayer of HS-5 cells, in serum-free DMEM at 37°C. After 48-72 hours, the CM was removed and centrifuged at 13,000 g for 5 minutes to remove cellular debris. The secreted protein was precipitated by adding 50 µl of 100% trichloroacetic acid (TCA) and 50 µl of 2% deoxycholate (DOC) into 0.5 mL CM and centrifuged at 13,000 g for 10 minutes. The pellet was solubilized with 1 M Tris buffer (pH 8.8) and run on denaturing 12.5% SDS-PAGE gel. Dilutions of recombinant human

HAPLN1 protein (2608-HP, R&D Systems, Minneapolis, MN, USA) were used for quantification standards. Cell extracts were made using TOTEX buffer, as described previously⁷. Equal amounts of soluble protein were run on denaturing 7.5% SDS-PAGE gel and transferred onto a polyvinylidene fluoride (PVDF) membrane (Millipore, Bedford, MA, USA). The membrane was then incubated with the appropriate antibodies. Antibodies used for the CM were against Myc-tag (clone 9E10, Santa Cruz, Dallas, TX, USA) and HAPLN1 (MAB2608, R&D Systems, Minneapolis, MN, USA). Primary antibodies to pSTAT1 (9167), pSTAT3 (9145), STAT1 (9172), and STAT3 (9139) were purchased from Cell Signaling Technology (Danvers, MA, USA), tubulin from Millipore (DM1A, Bedford, MA, USA) and actin from Sigma-Aldrich (A5441, St. Louis, MO, USA). Immunoblots were analyzed by enhanced chemiluminescence as described by the manufacturer (GE Healthcare, Chicago, IL, USA).

ELISA of HAPLN1 in HS-5 cell conditioned media

Pierce® Streptavidin Coated 96-well Plates (15120, Thermo Fisher Scientific, Waltham, MA, USA) were coated with 4 µg/mL biotinylated anti-HAPLN1 antibody (BAF-2608, R&D Systems, Minneapolis, MN, USA) overnight at 4°C. The plates were washed 3 times with TBS containing 0.05% Tween-20 and blocked with 3% BSA for 1 hour. After washing, the samples were incubated overnight at 4°C. Next day, the plates were washed and incubated with 2 µg/mL detection antibody (MAB-2608, R&D Systems, Minneapolis, MN, USA), for 0.5 hour at room temperature. Plates were washed and incubated with secondary anti-mouse HRP-conjugated antibody (95017-332, Cytiva, Marlborough, MA, USA) diluted 1:5,000 for 0.5 hour. After washing, TMB (34028, Thermo Fisher Scientific,

Waltham, MA, USA) was added to the plates and incubated for 15 minutes. The reaction was stopped using 1N H₂SO₄, and absorbance was measured at 450 nm. Dilutions of recombinant human HAPLN1 protein (2608-HP, R&D Systems, Minneapolis, MN, USA) were used for quantification standards.

Immunohistochemistry (IHC) analysis

Mouse tibiae were fixed in 10% formalin-buffered saline and decalcified. The tissue was paraffin-embedded and sectioned. Sections were deparaffinized in xylene and rehydrated in graded alcohols, and the epitope was retrieved by boiling in citrate buffer (pH 6.0; Vector Laboratories, Burlingame, CA, USA) for 20 minutes. Immunohistochemistry was performed using antibodies against CD138 (clone B-A38, Bio-Rad, Hercules, California, USA) and HLA class 1 ABC (ab225636, Abcam, Cambridge, UK) with the secondary anti-rabbit (Alexa Fluor® 647 Conjugate; CST4414, Cell Signaling Technology, Danvers, MA, USA) and anti-mouse (Alexa Fluor® 488 Conjugate; CST4408, Cell Signaling Technology, Danvers, MA, USA) antibodies. The TrueVIEW Autofluorescence Quenching kit (Vector Laboratories, Burlingame, CA, USA) was used according to the manufacturer's instruction before mounting.

Single-cell cloning of MM cells

Luciferase-labeled MM.1S cells or STAT1 knockdown MM.1S cells were generated by lentiviral transduction. The lentiviral particle was packaged by transfecting pLenti CMV Puro LUC (w168-1)¹¹, MISSION pLKO.1-shSTAT1, (TRCN0000004267) or MISSION pLKO.1-puro Control Vector (SHC001, Sigma-Aldrich, St. Louis, MO, USA), with

packaging plasmids (pCMV-dR8.91, and pCMV-VSV-G) to 293T cells. pLenti CMV Puro LUC (w168-1) was a gift from Eric Campeau and Paul Kaufman (Addgene plasmid #17477). MM.1S cells were spinfected for 60 minutes at 1,200 g in the presence of 8 µg/mL polybrene. Transduced cells were selected with puromycin, and the stable clone was selected by limited dilution and clonal expansion. RPMI8226 STAT1 and STAT3 knockout CRISPR/Cas9-edited cell pools were purchased from Synthego Corporation (Redwood City, CA, USA). STAT1 and STAT3 knockout cell clones were generated by limited dilution and clonal expansion.

Quantitative PCR analysis

Total RNA and genomic DNA from samples were purified by Trizol (Invitrogen, San Diego, CA, USA) according to the manufacturer's instruction. cDNAs were synthesized from the total RNAs using iScript cDNA synthesis kit (Bio-Rad, Hercules, California, USA). QPCR was performed and analyzed using a Bio-Rad CFX Connect real-time system. The absolute copy number of *luciferase* gene was determined by the standard curve using serial dilutions of the plasmids (pLenti CMV Puro LUC w168-1) as quantification standards for *luciferase*. The human-specific primer pair for *HAPLN1* was designed to target the PTR1 domain of *HAPLN1*. The primer sequences were Luciferase (forward, TGATTACACCCGAGGGGGAT; reverse, CTCACACACAGTTCGCCTCT), *HAPLN1* (forward, TCTCAAATTTCACGAGGCGC; reverse, GCTCTCTGGGCTTGATG), SMA (forward, GTGTTGCCCTGAAGAGCAT; reverse, GCTGGACATTGAAAGTCTCA), STAT1 (forward, CTAGTGGAGTGGAAAGCGGAG; reverse, CACCACAAACGAGCTCTGAA), STAT3 (forward, CCTCTGCCGGAGAACAG;

reverse, AACACCAAAGTGGCATGTGA), CD44 (forward, TGGCACCCGCTATGTCGAG; reverse, GTAGCAGGGATTCTGTCTG), SDF-1 (forward, TCAGCCTGAGCTACAGATGC ; reverse, CTTTAGCTTCGGGTCAATGC), and ICAM-1 (forward, GGCCGGCCAGCTTATACAC; reverse, TAGACACTTGAGCTCGGGCA).

Mining Algorithm for Genet/c Controllers (MAGIC) analysis

Differentially expressed genes between GST and GST-PTR1 samples¹³ were passed through MAGIC¹⁴ using default settings. Predicted transcription factors and coregulators were ordered by Score and graphed.

STAT1/3-dependent luciferase reporter assay

RPMI8226 cells were transiently transfected with Signal STAT3 Reporter Kit (CCS-9028L, Qiagen, Hilden, Germany) using Lipofectamine 2000 (Invitrogen, San Diego, CA, USA). The transfected cells were split into a 24-well plate 48 hours after transfection to control for the same transfection efficiency and treated with 100 nM MBP or MBP-PTR1 or 50 ng/mL IL-6 for 24 hours. Cell extracts were incubated with luciferin in a white 96-well plate, and the luminescence was measured by ENSPIRE plate reader (Perkin Elmer, Waltham, MA, USA).

Electrophoretic mobility shift assay (EMSA) and supershift assay

EMSA to measure STAT1/3 activity in MM cells were performed using ³²P-labeled double-stranded DNA probes with the following sequences: 5'-GTGCACATTCGGTAAATCGTCGA-3'. Cell extracts were made using TOTEX buffer

as described before², and extracts were separated on 4% native polyacrylamide gel, dried, and exposed to a phosphor screen (Amersham Biosciences). For super shift assays, 1 µL of anti-STAT1 or anti-STAT3 antibody (9172, 9139, Cell Signaling Technology, Danvers, MA, USA) was added to the cell extract reaction mixture before probes were added.

RNA-sequencing transcriptome analysis

RPMI8226 WT and STAT1 KO clone were treated with 100 nM MBP or MBP-PTR1 for 6 hours in 3 biological replicates run on 3 separate days (GSE237216). The frozen pellets were shipped on dry ice to Genewiz/Azenta (South Plainfield, NJ, USA) for RNA sequencing, RNA extraction, sample QC, library preparations, and sequencing reactions. Briefly, total RNA was extracted using Qiagen RNeasy Plus Universal kit (Qiagen, Hilden, Germany) following the manufacturer's instructions. The RNA sequencing library was prepared using the NEBNext Ultra II RNA Library Prep Kit (New England Biolabs, Ipswich, MA, USA) for Illumina using manufacturer's instructions. Raw sequence data generated from Illumina HiSeq. Reads were aligned to the Homo sapiens GRCh38 reference genome by STAR. Differential expression was analyzed using DESeq2 using count values and Likelihood Ratio Test¹⁵. Genes with an adjusted P value (P adj) of <0.05 were subjected to Leiden Clustering with a resolution of 1.0 using custom Python scripts utilizing the leiden tool in Scanpy (PMID: 29409532)^{16,17}. For each cluster, the mean expression and standard deviation were plotted per condition. Enrichment score shown in Figure 4D were calculated as follows. First, gene lists associated with each pathway in the KEGG database were compared to the list of genes upregulated with MBP-PTR1.

Fisher Exact tests for the overlap between lists were performed using custom Python scripts. On a cartesian plot of $\log_{10}(\text{Odds ratio})$ vs confidence (- $\log_{10}(P \text{ adj})$), the Enrichment Score is calculated as the Pythagorean distance from the origin to each data point on the plot:

$$\text{Score} = \sqrt{\log(\text{Odds})^2 + \text{confidence}^2}$$

HAPLN1 AlphaLISA assay on patient BM plasma fractions

Bone marrow (BM) aspirates from MM patients were obtained in accordance with the University of Wisconsin-Madison Institutional Review Board requirements (HO07403). Cytogenetic risk was assessed by fluorescence *in situ* hybridization (FISH). The plasma layer of patient BM aspirates was subjected to an amplified luminescent proximity homogenous assay-linked immunosorbent assay (AlphaLISA). First, the IgG level in each BM sample was measured using the Human IgG ELISA kit (BMS2091, Invitrogen, San Diego, CA, USA) following the manufacturer's protocol, with the dilution factor of 1,500,000. Plasma samples were diluted 50 times in PBS and final IgG level was adjusted by adding human IgG isotype control (31154, Invitrogen, San Diego, CA, USA) to match the highest IgG concentration among all the samples analyzed. The balancing of total IgG was necessary because preliminary study indicated that IgG was negatively interfering with AlphaLISA assay (data not shown). The standard was prepared by serial dilutions of recombinant HAPLN1 (10323-H08H, Sino Biological, Beijing, China) with standard diluent (FBS diluted 50 times in PBS with human IgG isotype control added to match the highest IgG concentration among the samples). The cross-reactivity was tested using recombinant HAPLN3 (H00145864-P01, Abnova, Taipei, Taiwan). The assay was

performed using assay buffer (25 mM HEPES, 0.5% BSA, 0.5% Triton X-100, 1 µg/mL Dextran) at room temperature. Diluted patient samples (5 µL) were incubated with 7.5 ng each of 2 primary anti-HAPLN1 antibodies, BAF2608 (R&D systems, Minneapolis, MN, USA) and HPA019105 (Sigma-Aldrich, St. Louis, MO, USA) for 30 min (15 µL total volume). The secondary rabbit IgG acceptor bead (6760002S, Perkin Elmer, Waltham, MA, USA), 1 µg in 10 µL assay buffer, was added and incubated for 1 hour. Subsequently, the streptavidin donor bead (AL159C, Perkin Elmer, Waltham, MA, USA), 1 µg in 25 µL assay buffer, was added, and after 30 min, the samples were measured by ENSPIRE plate reader (Perkin Elmer, Waltham, MA, USA).

The CoMMpass study data

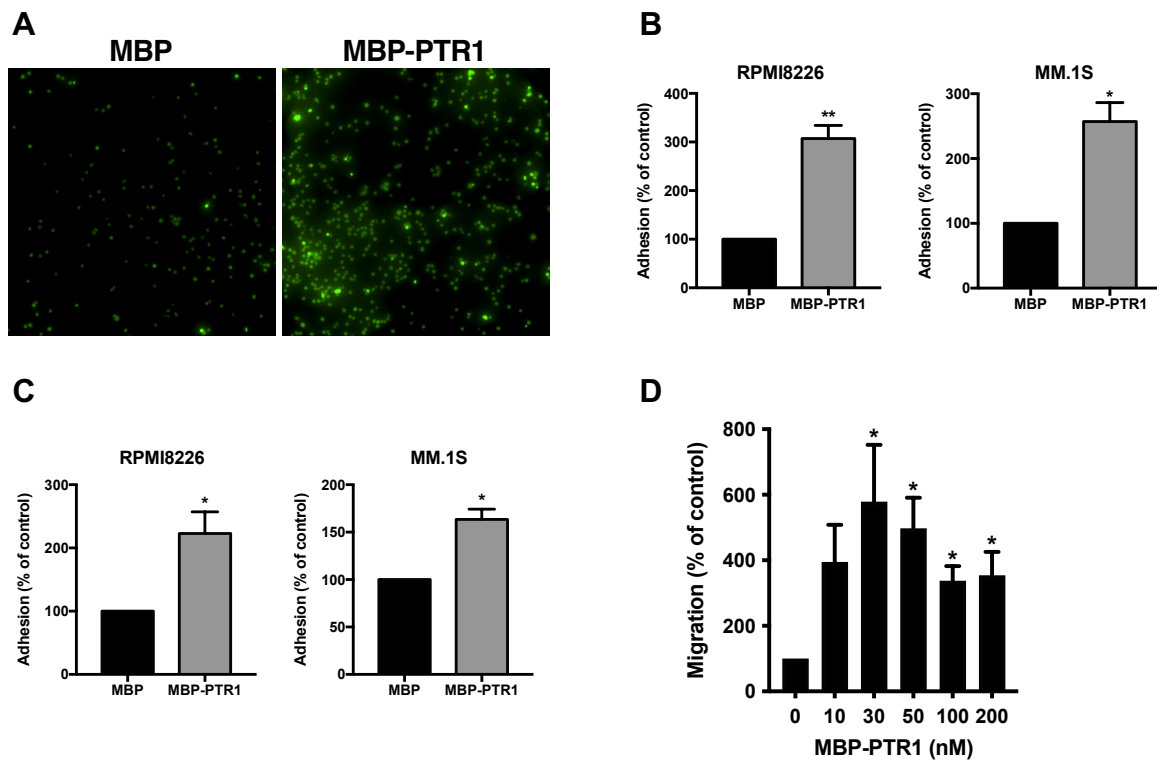
From the IA17 CoMMpass dataset, patients were divided into two groups based on their STAT1 mRNA levels using a TPM cut-off value of 96. The Kaplan-Meier progression-free survival (PFS) curve for the STAT1 high group (n=48) and the low group (n=47) was plotted from the Multiple Myeloma Research Foundation Researcher Gateway. These data were generated as part of the Multiple Myeloma Research Foundation Personalized Medicine Initiatives using the Genospace Population Analytics platform (<https://research.themmf.org> and www.themmf.org).

Statistical analysis

Statistical analysis was performed using the two-tailed Student's *t*-test. For the analysis of time-lapse microscopy, the two-tailed Mann-Whitney test was used. The log-rank test was used for the Kaplan-Meier survival curve. A P-value of <0.05 was considered

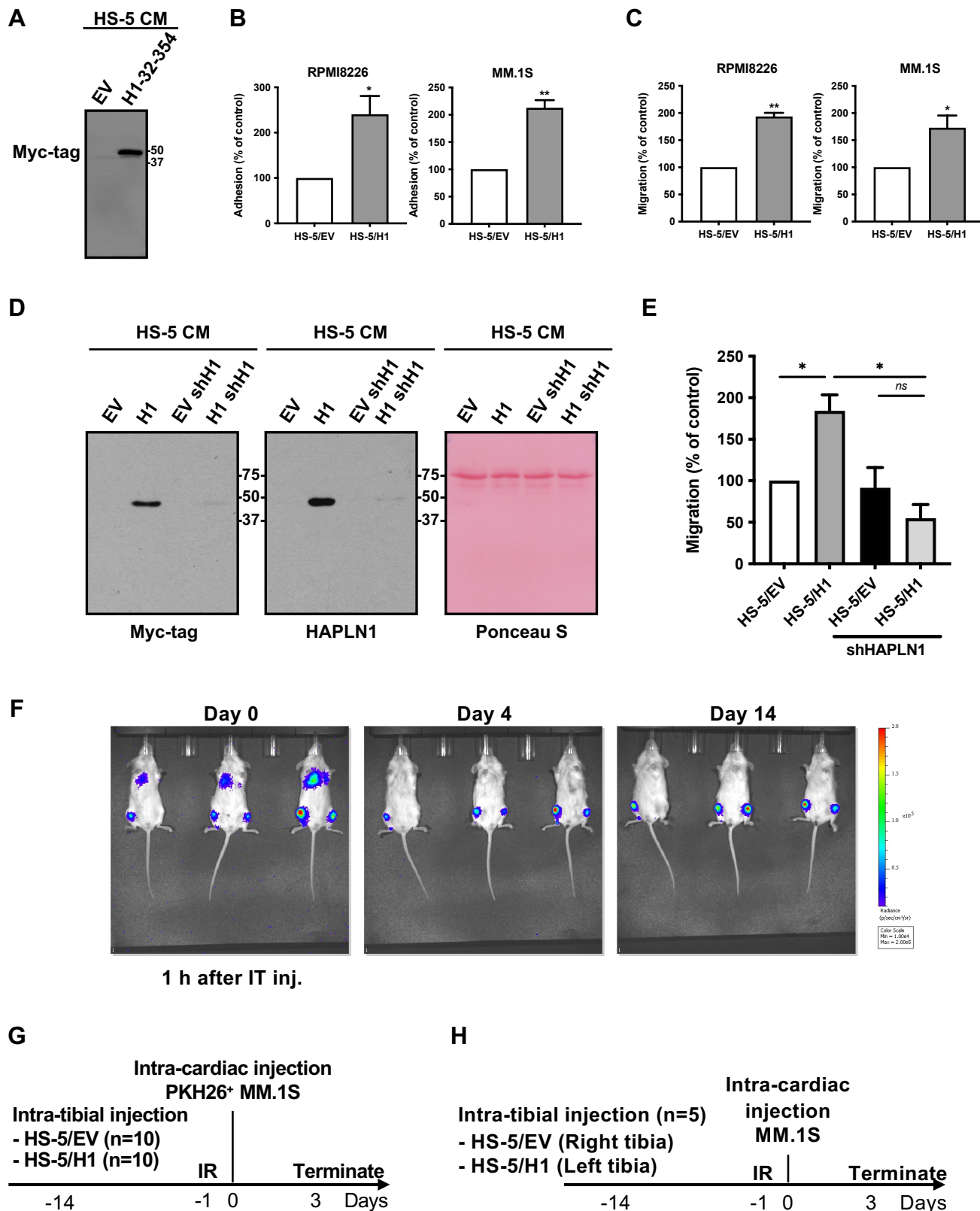
statistically significant. The analysis was performed with GraphPad Prism 9 Software (GraphPad Software Inc., La Jolla, CA, USA).

Supplemental Figure 1



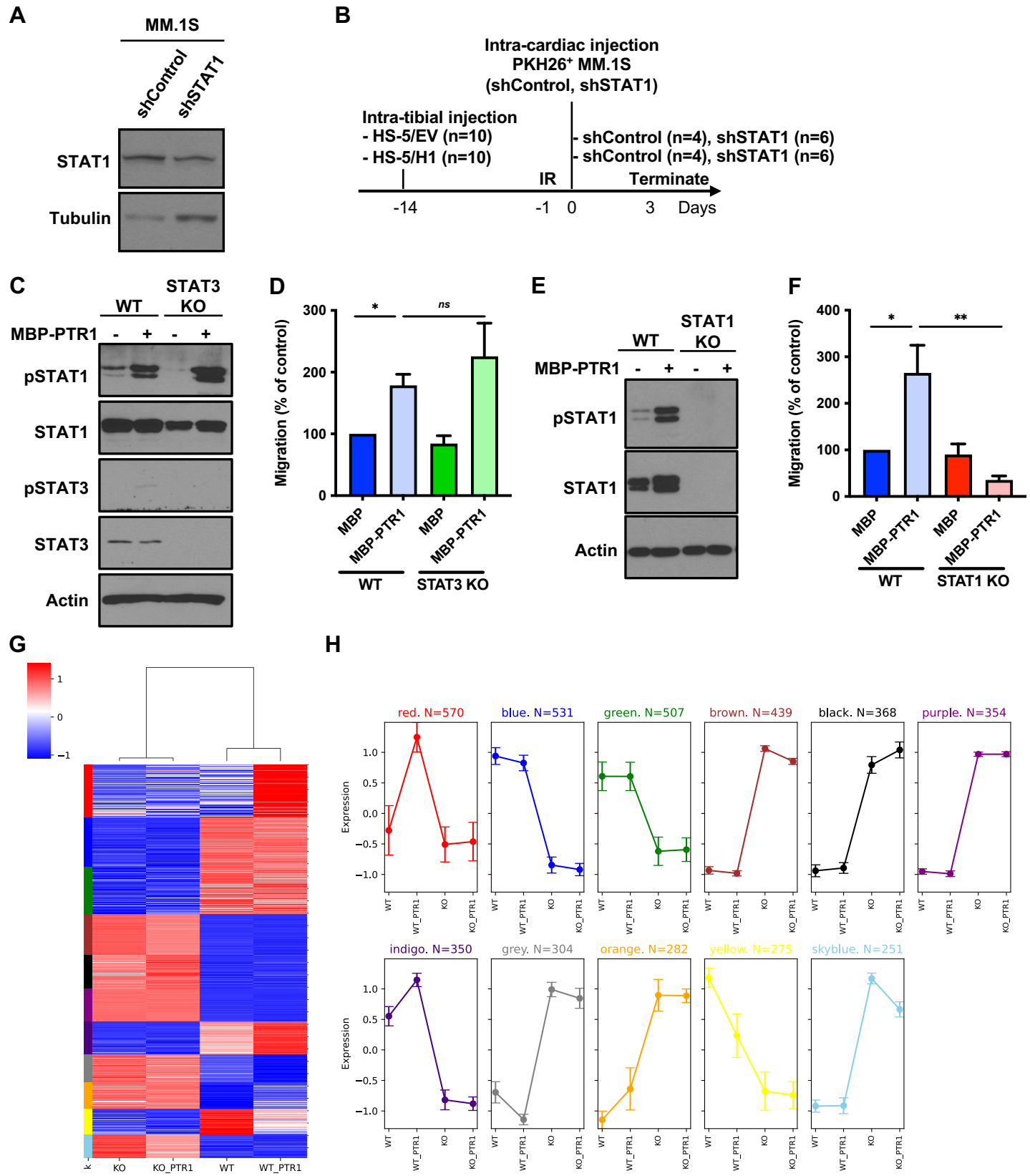
Supplemental Figure 1. HAPLN matrikine increases MM cell adhesion and migration. (A) Microscopy images of RPMI8226 cells adhered to fibronectin-coated plates following incubation with MBP or MBP-PTR1 at 100 nM for 16 hours. (B) Graphs depicting %adhesion of RPMI8226 and MM.1S MM cell lines in response to MBP or MBP-PTR1 (100 nM) normalized to MBP control being set as 100%. (C) Graphs depicting %adhesion of RPMI8226 and MM.1S MM cell lines adhering to endothelial cells (HMEC-1). MM cells were incubated with MBP or MBP-PTR1 at 100 nM for 16 hours prior to the adhesion assay. (D) Graphs depicting %migration of RPMI8226 MM cell lines in response to indicated MBP-PTR1 concentrations in the lower Transwell compartment with the control (0 nM) set as 100%. Experiments were independently repeated 4 times for (B, left) and 3 times for (B, right, C and D). Data are expressed as means \pm SEM. *, p < 0.05; **, p < 0.01.

Supplemental Figure 2



Supplemental Figure 2. MM cells adhere and migrate towards BMSCs secreting HAPLN1 matrikine. (A) Western blot analysis of the conditioned media (CM) of HS5/EV and HS-5/H1 cells using anti-Myc-tag antibody. (B) Graphs showing %adhesion of RPMI8226 and MM.1S MM cell lines to HS-5/EV or HS-5/H1 cells with control HS-5/EV cells set as 100%. (C) Graphs showing %migration of RPMI8226 and MM.1S MM cell lines towards HS-5/EV or HS-5/H1 cells in the bottom Transwell chamber with the HS-5/EV group set as 100%. (D) Western blot analysis of the CM of HS5/EV, HS-5/H1 and HAPLN1 knockdown HS-5 cells using anti-Myc-tag and anti-HAPLN1 antibodies. The Ponceau S stain is shown as a loading control. (E) Graphs showing %migration of RPMI8226 cells to HS5/EV, HS-5/H1 and HAPLN1 knockdown HS-5 cells in the bottom of Transwell chambers with the HS-5/EV group set as 100%. (F) Validation of BMSC intra-tibial (IT) injection. Luciferase-labeled HS-5 cells were injected via the intra-tibial route and imaged by IVIS on indicated days. On Day 0, 1 h after the IT injection, the cells were detected in the tibia and chest area, indicating the injection was rightly done in the bone marrow partially entering the systemic circulation. On Day 4 and 14, the majority of the cells were detected in the tibia and absent in chest areas. Of note, the first mouse was injected only in one leg showing that the majority of the injected cells remained within the injection site. (G) The experimental scheme for Figure 2A-B is depicted. IR refers to sublethal whole-body irradiation at 3 Gy. (H) The experimental scheme for Figure 2C-D is depicted. All experiments were independently repeated 3 times for (B and C, left) and 4 times for (C, right). Data are expressed as means \pm SEM. *, p < 0.05; **, p < 0.01.

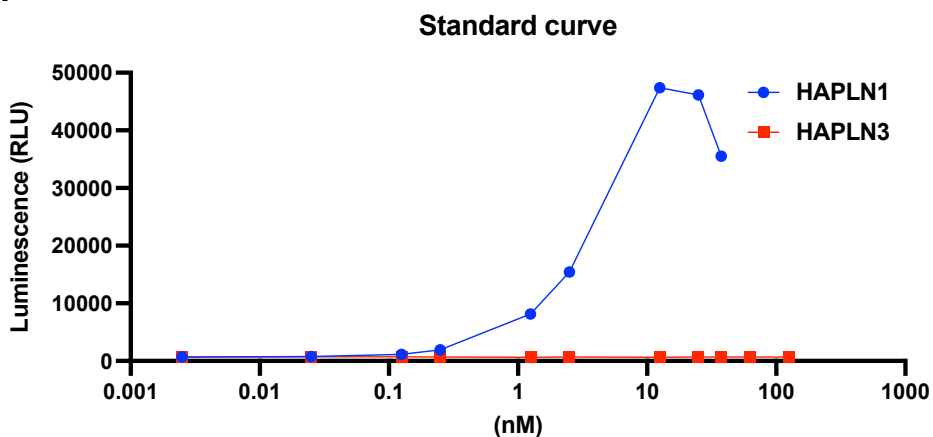
Supplemental Figure 3



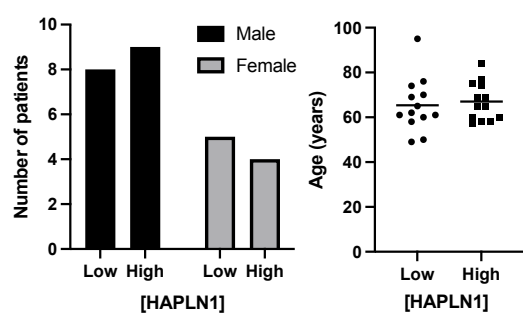
Supplemental Figure 3. STAT1 is required for HAPLN1 matrikine-induced MM cell migration. (A) Representative Western blot analysis on MM.1S shControl and shSTAT1 clones probed with STAT1 and tubulin antibodies. (B) The experimental scheme for Figure 4B is depicted. (C) Representative Western blot analysis of indicated proteins in RPMI8226 WT and STAT3 KO cells treated with 100 nM of MBP or MBP-PTR1 for 6 hours. (D) Graphs depicting %migration of RPMI8226 WT and STAT3 KO cells in response to MBP or MBP-PTR1 (100 nM) with MBP treated WT being set as 100%. The graph depicts the mean \pm SEM of the quantification of 3 independent experiments. (E) Representative Western blot analysis of indicated proteins in RPMI8226 WT and STAT1 KO cells treated with 100 nM of MBP or MBP-PTR1 for 6 hours. (F) Graphs depicting %migration of RPMI8226 WT and STAT1 KO cells in response to MBP or MBP-PTR1 (100 nM) with MBP treated WT being set as 100%. The graph depicts the mean \pm SEM of the quantification of 3 independent experiments. (G) Heat map of the cluster analysis on differentially expressed genes from the RNA-seq data. (H) Summarized bar graphs showing the 11 clusters. Data are expressed as means \pm SD.

Supplemental Figure 4

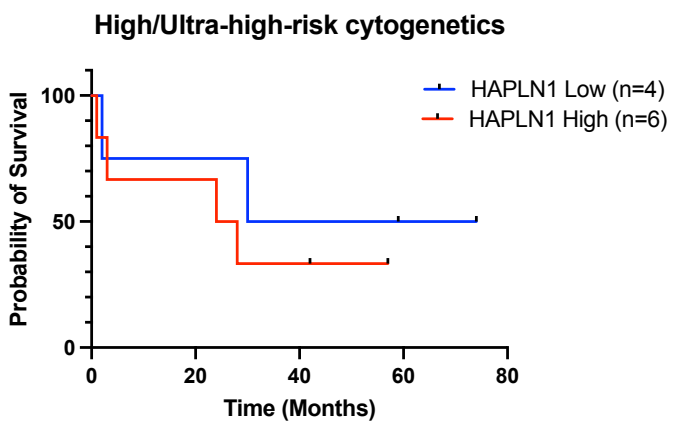
A



B



C



Supplemental Figure 4. Validation of the AlphaLISA specificity and NDMM patient distribution and outcomes. (A) The standard curve of recombinant HAPLN1 and HAPLN3 by AlphaLISA. Minimal cross-reactivity to HAPLN3 was observed in the assay condition even at a 10x excess concentration. (B) Graph depicting the distribution of sex and age in the HAPLN1 high and low patient groups in Table 1 and Figure 6A. (C) Kaplan-Meier PFS curve of high/ultra-high cytogenetic risk patients (n=10) separated by HAPLN1 levels.

Supplemental Tables

Supplemental Table 1. List of transcription factors driving genes induced by HAPLN1 matrikine in RPMI8226 MM cells as detected by the MAGIC analysis.

Factor	Critical ChIP	KS statistic	Obs Tail Mean	Exp Tail Mean	Tail Enrichment	Raw p	Corrected p	Score
NFKB	6.54530669	0.2807431	35.1815127	41.7137979	11.7715788	5.4838E-39	2.7419E-37	430.391889
RAD21	4.30659814	0.11932018	10.1861354	11.0218637	25.3766696	2.1641E-07	7.7288E-07	155.099407
EBF1	7.8215516	0.15116738	25.7923094	31.3995508	10.1996429	1.3202E-11	1.1002E-10	101.573573
STAT3	7.78945995	0.14549345	29.1684577	36.3924389	9.07545231	8.7938E-11	5.4962E-10	84.0381563
EZH2	3.234928	0.19419403	27.836516	42.5649865	4.77996018	7.085E-19	1.1808E-17	80.914256
PU1	5.1502342	0.12640798	21.2137543	26.3001862	9.34131066	3.0418E-08	1.3827E-07	64.0747377
BCL11A	6.04573148	0.19510129	34.7097976	60.9969861	3.64081475	4.7592E-19	1.1898E-17	61.6190477
SMC3	4.68696292	0.11820601	15.9878211	19.7357555	9.5315373	2.9157E-07	9.7191E-07	57.3071583
IKZF1	13.3526104	0.16147157	61.5964912	92.132544	5.03434535	3.5034E-13	4.3792E-12	57.1831243
NFIC	5.25073471	0.15884057	24.0940542	36.9950302	4.7352297	9.0533E-13	9.0533E-12	52.2920499
BATF	5.32278254	0.11676896	30.2658432	41.3692402	6.45163667	4.2654E-07	1.3329E-06	37.9046079
BCL3	6.74636988	0.15027822	31.9802883	54.6122743	3.82611419	1.7856E-11	1.2754E-10	37.8569144
RUNX3	6.88436818	0.08940377	16.8522973	20.3122718	10.7412841	0.00024567	0.00058492	34.7255065
ATF2	7.69754014	0.12822033	25.6187728	40.4857537	4.44639883	1.8086E-08	9.0432E-08	31.318997
FOXM1	9.40233713	0.12061475	27.6756415	43.302642	4.5420286	1.5251E-07	5.8658E-07	28.3044526
NFATC1	10.4608658	0.13996331	35.5513216	70.3858052	3.0411568	5.2064E-10	2.8924E-09	25.9676401
POU2F2	9.3629058	0.11167551	31.2612265	56.1340636	3.51368402	1.5822E-06	4.6534E-06	18.7357747
IRF4	7.16202006	0.10815998	32.0794635	56.8426282	3.59090176	3.7789E-06	1.0497E-05	17.8788679
MTA3	13.7923437	0.12081717	27.8578708	60.7333191	2.6947523	1.4434E-07	6.0142E-07	16.7635813
CTCF	3.8769406	0.07935412	8.98488556	12.4032665	6.25680765	0.00166003	0.00345839	15.3987952
P300	2.77437163	0.09329994	17.7171732	29.2440939	4.0740514	0.00011017	0.00027543	14.5035839
TCF3	8.40615591	0.09397206	30.5820316	59.3857147	3.12348063	9.5606E-05	0.0002516	11.2423342
TCF12	5.94150791	0.08057992	24.7672181	41.127701	4.0276879	0.00133106	0.00302513	10.1467778
MEF2A	6.40152359	0.07965557	36.4441096	61.4131955	3.91913847	0.00157276	0.00341904	9.66496958
CEBPB	4.80577895	0.05654477	15.4201692	19.9573499	7.79724699	0.05453822	0.08796486	8.23148166
MEF2C	8.11488021	0.076667621	49.6025755	92.4303226	3.31637567	0.00265794	0.00531588	7.54284723
NR3C1	7.80499919	0.06750732	38.5552027	61.4993591	4.36078626	0.01178554	0.02182508	7.24345863
PAX5	5.78318766	0.06938323	22.7943829	39.0947254	3.79679802	0.0088249	0.01697097	6.72144621
GATA2	6.03194	0.0578961	23.3087111	33.9277113	5.39000105	0.04581855	0.07636425	6.02122367
STAT5A	9.24860609	0.0580144	34.0913111	55.0467494	4.25369582	0.04511625	0.07778665	4.71775258
WHIPIGG	11.1504468	0.05871475	22.6731897	43.9084243	3.13543105	0.04114682	0.07347647	3.5551139
STAT1	9.55873538	0.0564272	91.9662042	179.162884	3.10939693	0.05536037	0.08650057	3.30522992

Factor	Critical ChIP	KS statistic	Obs Tail Mean	Exp Tail Mean	Tail Enrichment	Raw p	Corrected p	Score
FOSL2	6.30505182	0.05111308	28.7374882	48.1289744	3.96392838	0.10537763	0.15966307	3.1584404
GATA3	4.76647081	0.04636683	22.6681247	36.526847	4.27131523	0.17736656	0.23968454	2.64975298
PRDM1	11.7633149	0.05097104	79.2439249	194.289492	2.37760936	0.10711234	0.15751815	1.90843427
SUZ12	17.9117707	0.04947767	44.6274849	101.768764	2.56200512	0.12682015	0.18117165	1.90077663
CTBP2	13.1683098	0.0474254	28.4410465	59.8815696	2.80919677	0.15862874	0.22031769	1.84550358
ERALPH A	3.21758498	0.04414241	39.28017	73.4525153	3.29894494	0.22237142	0.29259397	1.76076116
STAT2	13.5089439	0.04344046	86.5307552	247.026163	2.07829571	0.23824257	0.30543919	1.07047866
FOS	3.40643612	0.03190816	14.1483213	27.1649798	3.17387915	0.61490065	0.76862581	0.36272689
ZNF217	13.1118749	0.02802284	39.2074186	82.1531593	2.82590487	0.76829368	0.93694351	0.07993522
JUN	4.90573319	0.02526052	19.2502293	32.7699553	3.84772477	0.86491446	1	0
JUNB	10.9873312	0.02004601	34.196361	68.4471157	2.99682379	0.97737302	1	0
RXRA	19.7756369	0.01234603	43.7135871	120.165459	2.14355832	0.99999508	1	0
BRF2	60.3457987	0.01171055	75.874739	459.308529	1.39576449	0.99999896	1	0
HDAC6	64.4782257	0.00920812	84.1928925	213.595371	2.30125626	1	1	0
NELFE	116.925782	0.0089239	85.8248167	283.754374	1.86722587	1	1	0
NANOG	33.3381245	0.00870787	47.5423245	131.385557	2.13407661	1	1	0
POL3	369.460895	0.0034495	53.9453836	550.874671	1.21711493	1	1	0
BRF1	299.394965	0.00412712	83.2064894	570.288768	1.34165271	1	1	0

Supplemental Table 2. List of genes in the cluster analysis of HAPLN1 matrikine induced genes.

Blue	Green	Skyblue	Brown	Red	Black	Yellow	Orange	Indigo	Grey	Purple
FAT4	IFI6	KCNMB4	THBS2	MARCKS	DDR1	UGT2B4	AK4	PTPRM	HAVCR2	ATP9A
RPS4Y1	PLSCR1	PRAMEF2	SIGLEC7	CD83	ATP2C2	SNCAIP	LIPG	ZFY	TMCC2	IGF2
MEF2C	LGALS9	FLNC	SMYD1	CXCL10	WNT5A	RNF144B	CRTC3	DIAPH2	ELFN2	CDC42EP1
MME	OAS2	TJP3	KIF1A	CD70	SCN4B	TCEAL8	PTPRK	EPHA3	DUSP4	PCARE
INPP5D	ERP29	TGFA	CLDN1	ADPRH	ADARB2	CYTH4	ABTB2	ZC3H12C	ARHGAP39	KEL
LINC01612	SRI	TPRXL	LGR4	MFSD2A	NXN	GULP1	CD59	SOX4	RXRA	SLC13A4
CTNNND2	HLA-F	MAP7D2	HABP2	TNFAIP3	SLC16A9	OR2W3	GJC1	GJA1	GPC1	MATN2
DDIT4L	STAT1	TMEM37	MAMLD1	TLR7	LIMS2	PYCARD	FARP1	CYBB	CLDN3	BMP5
CDH2	CCDC112	SMAD6	CCBE1	SIRPA	ELN	CRACDL	FOXP1	ADAMTS2	SPTLC3	MAGEA12
GALNT17	UBE2J2	GLI2	DAB2IP	TNFSF9	ATF7IP2	METRNL	KIDINS220	HRH2	MAL	FAT1
GALNTL6	MRPS26	F13A1	PYGL	GAS7	DPP6	NT5E	FN1	LCP2	IL17RC	EDN3
CTAG2	B4GALT2	ENTPD8	TMEM132B	PTGER4	LY6H	VSIR	ASAP2	SVIL	ARHGEF16	FBLN2
CTNNA3	COX17	LAD1	SLC47A1	IL10	ZNF423	DHCR7	APLP2	WWC3	KRT80	EPAS1
CDH4	CHCHD1	GLDC	LAPTM4B	TNIP1	FAM227A	SPI1	SIX4	CHRM3	WIPI2	CYP24A1
SLFN13	OAS3	ARHGAP22	SALL1	CD86	BIN1	ACSS2	IL2RB	ITPR1L2	GTF2IRD1	SCRN1
GLUL	HNRNPA1	GFPT2	RSPO2	RIPK2	FZD6	ACAT2	SGMS2	TFAP2B	ERMAP	DMRT3
SHANK2	TSPAN3	ST3GAL5	FREM2	TFRC	LINC01679	ARV1	ATXN1	KCNQ3	NOL4L	DMTN
SPON1	CIAO1	HLTF	GLI3	CD40	PKIG	EVI2B	CIZ1	PRKY	P3H4	PCOLCE2
TLR4	CYCS	PRXL2A	HSPG2	TRAF4	HOXB9	PLIN2	FOXC1	MIR4527HG	FBLN7	LAMA3
CD53	MAGOHB	CLEC18B	SYT12	DENND4A	AGAP14P	SS18L2	NHLRC2	EYA2	H1-0	ALX4
UTRN	ACLY	GSC	RASL11A	CDKN1B	CDCP1	TNFSF4	SFTP2A	ROBO1	ZER1	CD177
GLB1L2	PCNA	BBOX1-AS1	MYLK3	NRP2	MT1A	EPB41L1	SAMSN1	CNTNAP2	PLP2	TLCD4
SCAMP5	MX1	LIPT2-AS1	PLCB4	CCDC28B	PGLYRP4	H2AJ	ANO9	DPY19L2	KRT6C	IL1R1
LINC01432	CASP4	SH3RF3-AS1	FAM171B	PTX3	PRIMA1	TMA7	PDZD8	GRAMD1B	HDAC11	EMP2
LINC02506	IFI44	DUBR	IL34	MT2A	JDP2	EDA	PRRT4	DAPK1	RGS12	KLK1
KCNK1	AIP	PRAMEF4	UNC13B	ELL2	GRK3	NPRL2	BCL7A	SLC35F1	NACC2	RIMBP2
PARM1	ESRRRA	ERICH5	LINC00997	MAP3K8	OSBP2	NME3	HIPK2	PIP5K1B	RHOB	MPZL2
FCMR	PARK7	TUFT1	WNT7A	PELI1	TSPAN1	LSM10	ALDOB	IFNLR1	H2AW	EFR3B
SLC4A10	FH	ABTB1	NCKAP1	CD44	KIF19	CCDC86	ABCC4	MYO1E	MRGPRE	ACTL8
SERPINE2	DELE1	LAMB1	SOX13	RAB30	FGF17	TMEM258	ELF3	LONRF3	GAS6-DT	PRRX1
PGM5	ADA2	ALOX5	DNM1	MS4A7	ANKRD29	GCHFR	CMAHP	KIF13A	KIAA1522	GNG12
CD163L1	PPP1R8	FAM41C	NTRK3	CXCR5	ZNF827	NCK2	BASP1	TP53BP2	TSPAN12	OTX2
MEF2C-AS1	SELPLG	F2RL1	NAP1L2	PMAIP1	IGFBP2	APCDD1	TNS3	TGFB1	TTC39B	WFDC1
GCSAML	IFIT1	SLC6A3	CCDC88A	CD36	RORA	ARMCX6	STAT5B	MAP4K4	LGI2	MCTP2

Blue	Green	Skyblue	Brown	Red	Black	Yellow	Orange	Indigo	Grey	Purple
EFNB2	P2RY8	SDC2	OCLN	SGPP2	ZNRF1	CFC1	PALS2	CDK20	TMEM45B	WIPF3
BLNK	PSMG4	CHST14	NLRP13	VAV1	GRTP1	DMAC1	PHKA1	MTAP	PLXND1	ISLR
FERMT3	ACTR5	KCNMB2-AS1	MLC1	LINC02605	FAM43B	RPS14	TTC39C	ADGRE1	CREB3L4	DYSF
GNAI1	RBIS	DIPK1B	ZNRF2P1	DCP1A	CD300C	COMMD3	BNC2	PRPF38A	NEURL3	ANKRD18B
CD37	CBWD5	CALCRL	KCNT2	BCL2	PHLDA1	DPM3	CMTM8	LYSMD2	TSC22D3	DMRT1
SELENOP	MIEF1	GREB1	DGKB	C21orf91	SIM2	TEX264	THUMPD3	LHX3	PPP1R26	ZBTB7C
P2RX6P	EARS2	FGFR3	MAB21L4	PPRC1	LEF1	ANGPTL2	FMR1	CCDC71L	YPEL3	PCDH18
PAGE1	RCC1	IGLON5	TRIM9	ABI1	TNFRSF25	HRH1	ATN1	RCN1	LIMK1	CALML3
GMFG	SCMH1	KAT6B	TOGARAM2	DRAM1	INHBE	C9orf64	ST20-AS1	RUNX2	HBP1	MAGEH1
CARD18	MRM3	HOXB7	DOP1B	DMRTA1	EGFL6	SYVN1	RNF135	PEX5L	PTMS	OLFM1
ILDR2	SNHG4	ACSM3	DPY19L1P1	GRIA4	SEZ6L2	VIPR2	GPAT3	HEG1	VPS37B	MIR205HG
ABCG2	RAN	PINK1	CHRD	NOD2	SMIM35	NUDT2	SETD5	SPART	TUBG2	PITX1
CHN2	MIIP	MAPK11	MYO7B	IL32	SGK1	SQLE	CRACD	HDAC9	AGFG2	AKR1C1
BARX1	SSBP1	CRISP2	ESPN	RFTN1	DUSP9	UQCC3	SPSB1	SH3GL2	ADGRG5	CEP70
KLHL9	OAS1	PPP1R3B	ACOXL	PIM1	MELTF	AURKAIP1	CLIP2	DOCK8	FAM117A	DPYSL3
LY86	NETO1	MTM1	PXDN	PIK3AP1	FAIM	SEC24D	WNT10A	ETF1	NUAK2	BSND
MACROD2	CCDC57	KCTD11	TUBA1A	ZDHHC18	KLHL5	TRMT112	ZNF623	DMD	FGFR2	TMEM179
GPX7	SYF2	TADA3	HRK	CDKN2B	ARHGEF4	RBM38	WDR81	PDGFC	SHANK3	LINC01098
SAR1B	TTC13	BAIAP2-DT	PTPRE	HGF	SKAP1	RNASE6	CHIC1	TEX9	ST6GAL2	PPM1H
ZMAT2	XAF1	CCNI2	EBF4	IL12B	NFATC2	PLAAT3	FAS	EPHB2	CACFD1	PTPRJ
ANKS6	SAMHD1	TMEM270	MID2	IL7	MAPT	RPS21	RAB5A	G3BP1	NAB2	KRT81
ETS1	MACROH2A-1	HOXB6	CCDC144NL-AS1	CXCL9	LY6D	LAMTOR4	ARHGAP8	VAV3	MARCHF8	CELSR1
SERPINB6	ACSL4	OR7E14P	DBH	MIR155HG	ALS2CL	MTHFR	SOCS6	PPP2CA	BRD3OS	CSAG1
MSRA	GPD2	GPRC5B	PLEKHA7	CXCL3	ARHGEF10L	NDUFA2	MECP2	GEMIN5	ETV1	PPL
QPCT	ENO1	RHOD	CLIP4	TAF4B	OBSCN	FMN1	PURB	CBWD1	FUT1	ZPLD1
PTP4A2	ATP5F1E	PTPN9	TSC22D1	ACSL1	TMEM72-AS1	PGRMC1	BCL3	AMD1	ARID4A	TLE2
BRINP2	ITCH	SENP7	LPGAT1	IRF1	CHAC1	CD300A	ST8SIA1	CD28	TMRSS2	KALRN
LINC01192	DUSP23	RALGPS1	ERRFI1	SOCS3	NAT8L	TMEM50A	KIAA1671	CCDC88B	SHMT1	MTA3
PRKCB	XNDC1N	PSMG3-AS1	CNGB1	RELB	NSMF	SHISA2	SLC8B1	SH3RF2	BHLHE40	KSR1
IMPDH2	CIAPIN1	UICLM	PADI4	TNFAIP2	LINC02474	WDR82	LONRF1	FAM53C	ANO8	SATB2
CTNNA1	SLC5A6	C3orf18	DEGS2	IFNGR2	CCDC80	TMEM42	CBX6	UVRAG	MYCN	FYN
RBM47	RAB8A	KRCC1	CEMIP2	BCL6	FHL3	AIG1	TPO	GNB4	NDRG1	OLFM4
C3orf14	NCLN	SMPD5	LOXL1-AS1	NFKB2	ACOT2	EIF4E2	CXCL1	LPXN	ZYX	SLC6A8
CLTA	CD2BP2	GRHL1	PDGFA	CIITA	IQCH	UQCRRQ	CNOT10	RYR3-DT	CHST12	RIPK4
TOMM5	THOC3	F2R	RASSF6	RALGAPA-2	TESC	STX5	PLAU	IFRD2	CBFA2T3	STK32A
USP4	BCL7B	OR2C1	STRA6	PHAX	KCP	ARHGEF3	KIAA0232	COPS7B	CITED2	CPXM1
DCLK1	TMEM243	ANGPTL4	CD3G	STX4	CXCL6	MPV17L2	TAF1	AGTR1	FRAT1	SFRP5
FADS2	MAT2B	B3GALT9	MYO6	CXCL11	ACSM5	ENTPD6	BMF	CCND1	SLC25A45	SORL1

Blue	Green	Skyblue	Brown	Red	Black	Yellow	Orange	Indigo	Grey	Purple
PLEK2	MRPL58	CLIP1	ADAMTS17	NAMPT	LHX8	TMCO4	WDR31	ROR1	CLUAP1	OLFML2B
CNTN5	GPSM3	LIMA1	KCNH5	NCF2	TLCD5	SCP2	DUSP10	MS4A1	MAP3K9	KRT7
ABRACL	PRELID1	GTSE1-DT	PGBD5	IER5	CCNO	PRKCE	SMC3	PRKD1	PLAG1	MAGEC2
LHFPL1	TNFRSF1B	PCGF2	PKN3	B4GALT1	RNF43	LYL1	CD276	LRRTM3	ZMYM2	ATRNL1
TBL1Y	OXA1L	KBTBD2	GNGT1	NDE1	IL13RA1	ISYNA1	GCNT2	HNRNPAB	CSRP1	NECTIN2
IL3RA	PHC2	CCZ1	FAR2P2	STARD4	PDGFB	TMEM179B	ITGA6	LINC02484	SH3PXD2B	ZNF467
RNF182	USP18	ADAMTS1	RPS6KA2	RPF2	CSRP1-AS1	KRT40	RARRES2	RBMS1	HCG11	SFTPA1
ANTXR2	UBXN1	ZFYVE28	RALGPS2	NFKB1	KLK15	RTN3	S100A1	ANK3	PIP5K1C	KRT5
MAGI2	HERC5	GOLGA2	DNMT3B	MACIR	AMH	ATP6V0B	METTL6	SPP1	KCNJ4	NLGN2
CYSLTR1	SOAT1	CLDN7	SRPX	DOCK10	PRR5	SNU13	PPP1R12A	ZNF518B	RHPN1-AS1	ZFYVE1
TRIM58	KDM4C	DENND6A	TDRD10	C2CD4A	DNMBP	MRPS18C	FDXR	GPR137B	ATP2A3	SOBP
LINC02273	SDHB	H1-10-AS1	RASGEF1A	SEC24A	PTGES	HINT2	ANGEL1	NRIP1	FLYWCH2	C1orf198
JAKMIP2	PIGU	ABHD2	KRT17P5	EBI3	LINC02054	PEF1	REEP3	PLEKHG1	SLC6A9	SLCO3A1
TMEM273	PARP12	ADCY5	NUP62CL	PLXNC1	MRPS25	PAAF1	SUGP2	WDR36	TOR2A	ARHGAP23
ITGA4	PLGRKT	PRDM10	ZIC2	IER3	LINC02593	SH3BGRL3	ATRX	AK2	SLC16A14	ALDH5A1
ARMCX3	NDUFAF2	PACSin1	KCNJ12	ICAM1	SEMA6B	LTB4R	SLC49A4	SF3A3	CMTM7	CCDC190
LPCAT2	ANKRD39	ABHD8	ABCA3	SIAH2	MST1R	SP2-DT	TIAL1	ZSCAN20	TBC1D10A	SLC6A19
MYO10	PLAAT4	MAN2A2	CHST15	BATF	VGF	OCRL	NBPF15	APTX	BAIAP2	HTR2C
GTPBP6	SH2B1	LINC01503	CYP2U1	BTBD19	GPR157	NANS	SPECC1L	GCNT1	RCOR2	RHOC
CYFIP2	NADK	DOCK11	IQCE	ARAP2	EMID1	GRHPR	NF1	HERPUD1	FUT8	GRB7
PCSK6	PTPN1	ZRANB1	INHBB	CCL3	GATM	NREP	LRRC1	LCP1	NATD1	IL21R
RRAGD	ERVK3-1	VPS33A	FAM102A	RNF180	ADAM8	ALKBH2	ARL8B	POLR1E	ZBTB42	FAM178B
CPED1	ACAD9	WSB2	USP9Y	TASL	FOSL2	MRPS33	ZC3H4	CD74	SMTN	SLC6A15
LINC01480	NDUFAF3	LINC00938	CTPS2	DDI2	FAM120C	VNN1	TTC21B	NPM1	IL6R	CRAT
SSTR3	FARSA	PRTN3	SAMD11	HNRNPH1	ABI3	SPIN2B	MTMR10	DPH2	INVS	OTOG1
FADS1	PPIH	STN1	LINC00574	RAPGEF1	CCR2	TSPAN17	C21orf58	NR3C1	ABHD15	PDZK1IP1
ST3GAL6	AK6	BIVM	THPO	MAML2	OTUD7B	CDK2AP2	CBR3	LINC00623	CAPN10-DT	CERS3
RERGL	UCHL5	ENGASE	H2BC21	RASGEF1B	C2orf74-DT	SLC27A5	C2CD2	ACSL5	SH3RF3	CORO2B
HIGD2A	EPS15	NAA60	TJP1	HK2	HHATL	GNPDA1	TIGD7	ZNF98	LZTS2	KIAA0319
PRRCC1	UBE2C	LAMC1	CERS4	TNFAIP6	CMTM6	ARF4	RTN4RL1	RNF138	HERPUD2-AS1	A4GALT
TMX2	CRNDE	MYO9A	MORC4	IKBKE	CDH1	TUBB2B	KDM5C	RBM15B	SLC43A2	PAPLN
CCDC51	RILPL2	TTYH3	PTPN3	IL4I1	DZIP3	CDKN2AIPN_L	NECTIN1	ZNF676	PEX1	CGNL1
PSME2	METTL5	SYNE1	TBC1D16	PRRG4	EVL	RWDD1	CLU	YRDC	SPSB2	RAB39B
SERPINI1	DERL3	DYNLT2B	PPP1R13B	DEFB4A	ISM2	MGMT	C1QTNF1	RND3	LRP11	ARL4C
TNFSF11	CCDC12	IL18	PLA2G4D	NFKBIA	TMEM158	NXPH1	KIF26B	KMO	MOAP1	ZCCHC24
MS4A4A	DCX	TANC2	TUBB6	ALCAM	ATP1B1	CCDC127	TNRC6C	USP46	PLCG2	CERCAM
PRPF6	TRIM22	NBL1	KCNK9	LYN	MECOM	FKBP7	BRWD1	NXF3	COL9A3	LAX1
SMCO4	SNHG3	DTNB	SEMA3A	CCL4	ZBTB46	TMSB4X	JOSD1	PRNP	FAM210B	DLG5

Blue	Green	Skyblue	Brown	Red	Black	Yellow	Orange	Indigo	Grey	Purple
SPCS1	NECAP2	NECTIN3-AS1	TUBB3	JUNB	ITGB2	BTBD3	ITPR3	TAGAP	RAB20	PDXK
BTN3A3	ISG15	TFAP2A-AS1	NPAS2	NETO2	BCAS1	MRPL2	ANKRD26	CD47	RASAL1	PRAMEF11
MCTS2	TCFCP2	RAB43	EPB41L5	BID	SDHAF4	RPS27L	TOPBP1	MLKL	KLHL24	RIN2
DBN1	CYB561	ZNF594	ZMAT4	PLK3	LYSMD4	OSBPL11	ETS2	OGFRL1	ATP13A3-DT	KRT86
BRMS1	AKAP8	B3GNT4	NLRX1	OPTN	LINC02707	SVOP	JPX	DAPP1	IL10RB	ULK1
SLC25A6	HINT1	PNMA1	RASD2	MMP13	IL4R	CYSTM1	RAB27A	SZRD1	SPATA20	RAF1
LY75	TRANK1	BAZ2B	IQGAP2	NUP153	LINC00880	MGAT1	TCTN1	UBAP2	TRIM61	CCDC102A
BEST3	PELP1	LTBP1	YWHAZ	PPTC7	FOXD2	POLR2G	NKAP	SLC43A3	IFT27	ACVR1C
USP19	FCRLA	C13orf46	NCOA1	TET3	GPSM1	RPS3	KCNH4	EPB41	CIBAR1-DT	FHL1
SIGMAR1	SCAP	ZNF772	CDON	LYAR	LINC01967	SMIM26	CHM	ADSS2	PLEKHO2	LINC01016
MYO1F	MRPL33	FBXO32	FKBP9	CDC42SE2	KIAA0895	DOK6	MKRN2	HARS2	CCDC126	HES1
TRAPPC3	SLC35A4	RASGRF1	FXYD2	SRFBP1	TRIM16L	SDHAF3	TMEM63B	SPATS2L	MARVELD1	PNPLA5
UBE2D2	DHDDS	PAN2	MRC1	ZC3H12A	PPP1R3F	CSRNP1	BBS2	ATAD3A	TMEM164	CDH3
RER1	EFHD2	TNKS2	ESRP1	NUS1	GNB3	PARS2	PRKD3	LINC00944	PTGDR2	CTHRC1
RPL14	GLRX3	SLC7A11	RHOXF1P1	MDFIC	HMGN3	TMEM109	CEBPB-AS1	CLINT1	INAVA	ARHGEF11
SP140	GLRX5	NR2C2	DSP	USP1	TTC8	RAB3A	KCNA2	TOE1	HDGFL2	PRAMEF9
ZNF804A	BMI1	UAP1L1	PTPN12	BIRC3	ZNF558	CX3CR1	STS	MYEF2	TMEM117	ARHGAP15
WAS	TIMM13	SEMA3G	FGD5-AS1	TOPORS	LINC01674	SOCS2-AS1	NRARP	GPR158	DENND10	MAGEF1
FAR2	HSPA1A	LINC02561	TIMP2	NFKBIZ	IGFBP6	ELOF1	RGS16	EMC1	TBC1D9	DBH-AS1
GPAT2	ERH	SLITRK5	FAM133A	SOX2	CACNG6	FDFT1	SEL1L3	NOP16	AJM1	FER
EXOSC3	RPL35A	GPR107	NOTUM	RAPGEF5	FSCN1	MFSD12	GCNT4	RYR2	SLC7A7	ECI2
SLC16A7	POFUT1	MC1R	MARVELD2	OXSR1	PLEKHG3	TMEM59	WDR90	PLAA	TOM1	CNN3
PLEKHG4B	PSMC5	CLDN9	CHEK2P2	ZBED1	TMEM184A	ADRM1	PHYH	LGALS8	SNX30	PLD4
LY9	PDCD2L	TBC1D19	PPP1R14D	STARD5	SDC3	SRP68	PHF2	FAM111B	TOR4A	EFNB1
SORT1	EMG1	ERBIN	UNC119B	PUM1	LRRC75B	NXT1	RAB11FIP3	SLC36A1	FAM107B	LARGE2
STARD3NL	HID1	CCDC186	PLCD3	PIK3CD	GNGT2	ADRB2	BRPF1	PRELID3B	HBA1	FAM169A
SYNDIG1	DMAC2	ANKRD28	H2AC11	INSIG1	NCS1	FUZ	DYRK1A	TTI1	S100A11	BHLHE41
MTHFD2L	DNAJC12	MIAT	CRYBG3	RUNX3	TRAF1	ZNF672	MCM3AP	CDC25A	TMEM9	PTGS1
CAP1	DLGAP1-AS1	KDM6A	FANCD2	ZRANB2	B4GALNT4	SHISAL2A	HIVEP3	RBM22	PRIMPOL	LINC01315
CKAP4	SLC35B1	KBTBD7	MLF1	SLC25A24	CDK18	CAPG	RASSF5	CCNJ	ST3GAL4	ZNF319
BCAT1	UBE2B	VAMP4	LINC02910	ROR2	MAGEA3	SDF2L1	WDR44	TNFRSF14	ADM	SLC15A1
SLC17A9	TRMT2A	SWI5	OPRD1	TFAM	SECTM1	BLK	CUL9	ATAD3B	ZNF385A	ASPHD1
UGT8	CAPZA1	DPY19L2P3	TIMD4	CEP85	KCNK12	DRG1	ZBTB10	ZNF22	PRPSAP2	ENTPD2
TRIP6	NIPA2	SYNE2	UTS2R	EPOP	TPPP3	OSTC	CAV2	CA8	PIK3CG	SULT4A1
MRPL22	GNAS-AS1	SLC2A12	APP	CSF1	TREX2	CRIP1	PPFIBP1	DHX37	ZSCAN30	JDP2-AS1
COX20	POP5	DPY19L1	MAST4	CASP3	SH2D5	VEGFB	GSE1	COA7	PLEKHH3	ELFN1
PRELID2	POLR3K	TCP11L2	NLGN1	GADD45B	CFAP157	SLC52A2	FAM230C	HSPA9	ATP2A1	TXNRD3
MYL1	LARS2	MTMR2	ADARB2-AS1	CRACR2A	ZDHHC11	NAT14	TP53INP1	TM9SF4	ACP6	RAB31

Blue	Green	Skyblue	Brown	Red	Black	Yellow	Orange	Indigo	Grey	Purple
RUFY1	PHAF1	ZNF606	FBXO43	SLFN5	GRAMD4	TRIAP1	TSPOAP1	PSMB2	PAQR4	BCAM
HMGXB3	FOXP4-AS1	ATG7	MGAT3	TPTEP2	APLF	TNFRSF17	SDCBP	FCHSD2	ZBTB7B	NANOS1
ZNF257	MYL12A	ARID3B	GDNF	SERBP1	HECTD2	CYB561D2	RFC3	ZNF639	SIRT3	AIF1L
MFN2	TXNDIC15	CITED1	SPINT1	DCK	CD48	MAPKAPK3	SBF1	NFX1	ABCD1	SLC4A4
SLC15A3	DTNBP1	OSBPL5	SLC12A6	ATP13A2	FABP6	TMBIM6	GART	PDCD11	TBKBP1	ASB9
PTER	PDCD6	PATJ	LINC00957	RPIA	ZSWIM4	SPATC1L	CACUL1	NOC2L	SLC16A3	NPTX1
IMMP2L	TNFRSF13B	LRRC37B	EIF2AK1	LTB	THEM5	USP7-AS1	CYP1A1	RCL1	SIGLEC9	CCR10
FAF2	BMP6	TOR1AIP1	IRX4	GRPEL1	FUT2	VPS51	ANKRD11	DNAJC6	ZNF821	LINC00242
APBB1IP	ISOC1	MMP25-AS1	CEP170B	YWHAG	ANKRD36B_P2	ACTR8	MTUS2	HNRNPA0	CERK	DHX32
CSTPP1	CAP2	RLIM	SYTL3	CCR1	C15orf48	ZNF675	VDR	NSUN4	BBS9	GNG10
TSPAN7	EBLN3P	SPTB	TRMT2B	ZNF253	NUPR2	RPS26	MACF1	SLC25A33	TSR2	BCAR1
EIF2B3	KLHL6	CKAP2L	MAGEA6	ANKRD33B	CRIP2	TNFAIP8	TGFBR3	MAX	LINC02341	ACTN1
MRPL36	RPSA	S100A9	AOC3	PPM1K	ADAM19	KRTCAP2	PCYT1A	FOXJ3	KIFBP	SH3TC1
RBBP4	SMPDL3B	PAPSS1	KLHL42	CXCL8	RUNX1	TMEM223	PROSER3	GOLT1B	CBX8	FAM3B
SSR1	SNHG21	MAMDC4	FRMPD3	ANKRD30A	GPR153	ATP5MC2	PBX2	TSPAN5	GDPD5	PECR
OSBP	MAPKAPK2	S100A13	COBL	PSD3	NEIL2	EXOSC1	SPAG1	SIDT1	CCDC122	CLDN4
IK	CCT5	NEO1	UBE2QL1	NIBAN1	LINC02870	KLHL21	AHRR	PHF20	PIK3R3	ACADVL
LILRB4	TIMM22	RRAGB	ZFPM1	SH2D3A	CDC42EP4	TRIM52-AS1	OLIG2	EBNA1BP2	SRGAP2D	H2BC11
VDAC1	DDOST	UBP1	AAK1	SELENOT	RGL3	PLPP2	KIAA0753	EXOSC10	ABHD4	ARRDC1
HEMK1	RAD51B	USP28	MAGEB2	OXTR	PNPLA2	INTS5	ADM2	FBXO38	EGLN3	SUMF1
CANX	CYP27B1	SLC2A3	HERPUD2	MMD	TSPAN9	SEC22C	HSD17B1-AS1	CHSY3	FUCA1	GADD45A
SEC61B	CRLS1	APOL4	ADAM22	UTP23	LINC02253	DTWD1	CARD9	SFPQ	ZMYM3	COL18A1
YIPF5	COMMD10	SYP	ODAD3	B3GNT2	GRIN2C	SSU72	SUN1	DCAF1	TP53INP2	CRACR2B
TKT	APMAP	KRT17	MYO7A	CHSY1	LINC01805	ABHD14B	PINCR	DHX30	TMEM65	ZNF542P
SPCS2	RDH11	FCGR2A	SLC25A43	RAPH1	KCNJ11	RPP25L	PCNX4	C1orf109	HCFC1-AS1	CYTH3
TMEM201	SART1	FBXL18	MAN1C1	NFE2L3	FAM83H	SMIM30	BCOR	LINC01145	ZNRF2P2	ILF3-DT
CREB3	LSM11	TBC1D12	AKR1C3	SETBP1	TEAD3	RPL36	SIK3	CTSS	CLMN	FAM124A
TTC1	APOBEC3G	MIB1	ITSN1	IGFBP3	SHF	PREB	MIR503HG	RELA	MAPK3	PLXNB2
NKX2-1	FBXO6	RTL10	LINC02257	WIPF1	FNBP1	EEF1D	CDKN1A	FAM193B	MKS1	ADAM11
TRIM44	ALYREF	HDAC4	PALLD	HNRNPU	SLC16A13	DHCR24	ASB1	WDR77	EPS8L1	MANSC1
UBA7	RNF121	ATXN3	SH3BP4	PPIF	HTATIP2	PLA2G15	TNFRSF10D	LINC00869	RETREG2	SAYSD1
YOD1	KHDRBS1	CARD10	NUP210	SBDS	CDC42BPG	LIN52	RABGAP1	TTC4	ODAD4	SORBS3
PSMB9	MMP24OS	MIR4664	PDE5A	ELOA	WDR59	FRMD3	ATAD2B	GIMAP6	BTBD2	GSTZ1
CD33	RBFA	ANKDD1A	GK5	RNF11	LLGL2	ALG5	SH2B3	AKIRIN1	NIPSNAP1	SLC44A3
TIMM10	BTN3A1	SLC51A	CDK16	NEDD4L	ITGB4	ALG12	GATD1	SEMA3C	BNIP3L	RPS10P7
SEC22B	DPP3-DT	FBXL3	CCDC74B	FMNL3	TEP1	FDX2	CNTNAP1	KAZN	CCNG2	CSTB
STPG1	ELOC	TMEM210	EML5	IFIT3	NPHP3	MYLIP	RBKS	PARP8	RTN4RL2	SCHIP1
CTU2	ATP5MK	MOB1B	HERC2P4	APOL3	MKRN9P	SLC50A1	EML2	NOL7	CTDSP1	PPP4R1

Blue	Green	Skyblue	Brown	Red	Black	Yellow	Orange	Indigo	Grey	Purple
IL12RB1	GNB1	CACNB1	ADCY9	CSNK2A1	POMC	NDUFS4	PHF21A	GGA2	SNX29	SLC27A2
NADSYN1	PSMB8	TRAPPC6B	SKAP2	ZNF267	IQCG	CUTA	GRB14	IFNG-AS1	KRT16	YPEL5
LRRC47	TRMT6	PPP1R12A-AS1	FURIN	IL2RA	MAPK12	PCYT2	TSPAN33	TMEM138	RAD17	LINC01139
APBA1	RUVBL1	LNP1	CEP128	ZFP91	LRG1	FMC1	IRF8	ERLIN1	ZNF836	CSRP2
LARS1	RASSF3	PRDM5	DCLK2	TNFRSF9	CFAP36	SLC25A20	TFE3	SCML1	GATD1-DT	ADAMTSL2
RUBCNL	MRPL47	ZNF429	MICALL2	FAM3C	EMC3-AS1	ATP6V0E1	SEPTIN7	DNAJA1	SH2D3C	ADGRB2
PTMA	ELOVL1	CAMK2N2	MTURN	GTPBP1	COX6C	RPL23A	MAP7D3	CTPS1	PC	EPN2
IL24	HLA-B	ADAM10	BCL9	PGLYRP2	CARMIL1	RPS13	NCOA7	DPP4	ATP23	PCNX2
ARHGAP17	CSNK1G3	P2RY1	SCCPDH	NUAK1	LCAT	SLC25A38	APOBEC3B	WDR55	MCOLN1	RERG
CPNE3	POLR3F	RHPN1	SPIRE1	LARP1	SLC12A4	RPS25	SLC9A1	CLCN6	DSTNP2	LAMA5
CAMK1D	CLNS1A	TAB2	DBNDD1	QKI	MIR548XHG	DPYSL4	PITPNM1	PPP4R1L	FAM214B	KRT13
ZC4H2	MRPL48	TUG1	TBC1D8	TRIP10	SH3BGR	SRC	CDK13	ADPRS	LINC01003	ACP3
UBAP1	COX5A	PTPN21	NOXA1	RAB11A	MARVELD3	ZFP69B	ACTR3C	GIMAP4	LRRN4	EHD3
PLAC8	NFIA	ZHX3	TTC3	CXCL12	LINC02188	CPTP	FBXW2	THG1L	HAGH	AOPEP
EXOSC7	LZTFL1	IRX4-AS1	CRTAP	SMARCA2	CBR3-AS1	MORF4L2-AS1	OSBPL3	TMEM69	FAM167A	PCTP
EAF2	EXOC3	DDX53	DOCK6	CEBDP	IVD	FAM89B	MED12	OXR1	CAPNS1	STMN3
DCAF12	TIPIN	MXRA7	FZD7	PIM2	KIFC2	TNFAIP8L2	RASSF2	HBBP1	FAM78A	CFD
OLMALINC	NDUFB6	SUPT20H	TFDP2	HAPLN3	AMDHD1	RPN1	RBSN	UTP11	KIAA0895L	TMEM231
COA4	CDKN2A	YJEFN3	DLG3	WDR3	SPESP1	BET1	LRRC37A4P	UIMC1	CCM2	AQP3
SLC25A46	MX2	SPEN-AS1	FHOD3	TICAM1	RP9P	RPL19	PCM1	ZNF729	XKR3	BTK
MRPL20	PHLDA2	ARMC8	PLXNB1	HIVEP2	CREB3L1	CYB5B	CUX1	EEF1E1	RNPEPL1	CACNA2D2
ATP10D	NIFK	CBR1-AS1	ACVR1	ARHGEF40	C16orf74	ZCCHC17	C8G	PRKAR2A	PLEC	RNLS
REEP5	TXNDCC11	NCOA2	MFHAS1	CCL2	DNAAF8	SEC31A	CNTRL	TDRD7	ENKD1	PANX2
TFB2M	ANO7L1	VTI1A	LINC02064	PITPNB	HOXB4	MPG	B4GALT5	GRWD1	KDM7A-DT	COL4A4
ESYT2	MRPL1	SEPTIN3	LINC02983	GFOD1	TCTN2	PLPP5	EPHA10	RRN3P1	CD72	CFH
NFYC	YBX3	ZBED3	IER5L	AIM2	URGCP	ZFP42	KREMEN2	MCUR1	SCN9A	TNRC18
LINC01606	LAMP3	AEBP1	FAM214A	GSPT1	GINM1	TMC5	NONO	KCTD5	THRA	HEXB
C1orf174	WDR4	RWDD2B	EXT2	MYBPH	EEF1A2	MPC1	CENPE	SP110	TMEM254	LINC01414
DNAJC15	MRPS15	HSPA2	ATE1	SNX20	EGFL7	RPS5	ADD2	ARIH2	TIGD3	NUDCD3
GNE	MMADHC	RAPGEF2	DENND6B	NDUFAF4	INSIG1-DT	MINCR	TRNT1	GALT	NT5DC1	FGFR1
IFI27	ZFAS1	IFT80	C3orf33	TGIF2	SNX8	CHAMP1	TRIP11	ATG12	CCDC50	H2BC4
LARGE1	PFKP	NEDD4	SSBP2	IRF2	DNASE1L3	NOP10	IFNAR1	SMU1	KANK2	LXN
CPSF7	TFAP2C	CENPF	OAT	PSME4	TMEM260	BEX1	MKI67	AKAP17A	CLSTN3	ZBTB4
DPM1	LINC02864	C10orf88B	TRNP1	FAR1	CIB2	MRPS18B	JMY	GIMAP2	ASTE1	EDEM1
COMT	EIF2B4	RNF215	MANBA	ZC3HAV1	SLC27A1	ZFP69	ITSN2	TWNK	CALM1	NFIX
MRPL16	ZNF232	TCP11L1	ZNF318	WWC1	CHST2	ATG4C	NKIRAS1	DDX41	LINC02982	HAACL1
ZMPSTE24	UBE2L6	SETDB2	ZNF322	ID2	HSPA6	GORASP1	TMTC1	ZC3H15	ERCC2	SPIRE2
MAGOH	PPP1CA	LINC00662	PHACTR2	IRF9	FHIP2B	BANF1	NCOR2	TMEM106A	ST14	ABCB9

Blue	Green	Skyblue	Brown	Red	Black	Yellow	Orange	Indigo	Grey	Purple
ACO1	ZNF385B	RNF103	EVC	C12orf29	ZNF844	MEA1	MPHOSPH9	CHCHD3	MNX1-AS1	SPIN3
RFT1	BRD8	FOXD2-AS1	ZBED5	MASTL	PFN2	DHRS1	DUSP5	PDE3B	MCM5	TALDO1
RNF145	ABHD5	DYNC1H1	GARS1	ZFP36L1	RTL8A	ZNHIT1	ADCY1	CMPK1	BAK1	RBFOX1
PAM	ERAP1	SMC2	RAVER2	CEBPZ	RGS10	CARD17	TCAF2	CCT2	TKFC	BICD1
MRPL49	MARCHF3	LMTK3	LINGO3	PUM3	PDK3	MRPS34	CELSR3	KCNQ5	USP51	STRADB
DRG2	GNPDA2	MRTFB	LANCL1	EYA1	SLC9A9	TTC22	NIN	HAUS6	PIERCE2	IGSF9
QPRT	JPT2	PAK6	ARHGEF12	CLK4	CHD3	MEAF6	SLC25A25-AS1	KANK1	INPP5K	H2AX
CDC23	FAM32A	LGALSL	TFAP2A	CDK6	ACTR1B	PRANCR	CUL7	TPD52	SERTAD3	PMS2
MIX23	MUTYH	ZFYVE16	PRRT3	IKZF1	IL2RG	NUDT22	AMMECR1	BRD9	BRF1	CCDC69
YTHDF2	SNRK	SNX12	HIBADH	AHCTF1	TNFAIP8L1	NAT1	CEP350	UTP6	TYSND1	SMKR1
ZCCHC7	MBIP	STARD8	C22orf46	IL15RA	PSPH	UNC5A	SEPTIN7P2	ZDHHC5	STBD1	IQSEC1
UAP1	PPP1R14B	CLASP2	ABLIM1	TOP3A	CSNK1E	SLC7A8	TPST1	DEGS1	PSAT1	PLEKHB1
ZBTB8OS	POLR1C	SPTBN1	ENO2	NOL11	RYK	GMPPA	SLC25A53	GAR1	OSBPL6	SLC35G1
DUSP7	NSA2	GDPD3	ACER3	EIF4H	MESP1	RPL26	PPP1R12C	SNRPB2	CASP6	XXYLT1
MED24	EEF2KMT	ZNF714	TSPYL4	KDM2A	LGALS2	RPL28	C1orf21	SREK1IP1	ZXDC	CD4
ARMC6	C18orf21	BRWD3	WNK2	TIPRL	AKR7A3	RBM33-DT	MPRIP	TIMM17A	MKLN1-AS	GLS2
MRPL21	PFDN6	NHLRC4	CAMKV	KPNA6	SLC26A11	FNBP1L	UTY	MNS1	PHYHIP	SERAC1
MANF	SCNM1	EPG5	ID1	GORAB	SLC30A4	VAMP1	LARP4B	LIMD2	ZDHHC4	RSRC1
DMKN	PCBP4	APOOL	NRDE2	FRMD4B	LINC00920	TMEM70	MREG	CPNE8	RXRB	ALDH3A2
SEC23B	LSS	IGF1R	LDAF1	RAB21	C4orf36	RNF207-AS1	FLOT1	MRPS30	TOX2	ADPRHL1
PODXL2	B3GAT3	AVL9	DIP2C	GCH1	U2SURP	SPTSSA	SH3BP5-AS1	SFXN1	MIEF2	CLCN5
ARHGAP30	NUB1	KIAA1109	FMO4	WBP11	MIF4GD-DT	RPL18A	ANKRD10	DENND1B	PIGC	OTUB2
TOMM22	MIR3667HG	CPD	MAPRE3	SYNCRI	FBXL19-AS1	TMEM101	CASP8	NUFIP1	FZD1	PCCB
JCHAIN	HSPA4	SIPA1L2	AFAP1L2	COMMD5	CMTM4	ABCB6	GDI1	MIR646HG	MEF2D	LTBP4
LINC01194	SRSF4	CD109-AS1	CEP68	ZNF598	PTBP2	CEP41	ASAP1	HMGCS1	ORAI3	MBTPS1
ZNF296	ARFGAP3	H2AC17	ITGA3	BCL2A1	ATP6V1E2	RPS12	SHOC2	MTA2	RTN4IP1	BRD3
PGD	PLAAT2	SLC38A6	CAPN7	LINC02397	TFCP2L1	PRMT5	DTNA	SDHD	ZNF395	DONSON
SNRNP40	BST2		FBXO3	PIGV	ETFDH	AKIP1	EPIC1	PNRC2	ARL15	XPC
MORC1	RHEB		ZNF12	YTHDF1	H4C14	RPL41	RDX	PWWP2A	PIP5KL1	DIRAS1
DDAH1	SHFL		NUMBL	MPI	BBC3	MRPL43	KLHL11	RAPGEF6	FRAT2	SHANK1
SNX2	PPIE		PIK3CB	DUSP2	TXNRD2	RPS16	CREBBP	FBXW11	TRAM2-AS1	LRP1
TBC1D9B	PPIP5K1		AKR1C2	SVIL-AS1	NSMAF	TRPM2	STX6	TIGAR	MISP3	CD151
RPL26L1	NASP		EFNA5	CD274	TBXAS1	RPS15A	PDCL	NME6	MXD4	ZNF516
ERGIC1	SORD		INKA2	SLU7	LINC01655	MIEN1	VHL	LUZP1	H1-10	TMC8
LRRC59	SUB1		CRBN	NCOA5	LINC02444	RBM4	VPS41	HNRNPR	SDC1	BTG2
RPL11	SLC15A4		SELENON	MB21D2	PLEKHF1	IDH3G	ADGRL1-AS1	CHMP5	CD63-AS1	CXCR3
RPL22	THNSL1		KAT2B	CTNND1	BICDL1	AP3S1	SETD1B	PPIP5K2	PJA1	ZNF219
HIGD1A	GNAS		L1CAM	NOL10	PPP1R16A	MRPL10	LRRC8B	ZCCHC10	C14orf93	FEZ2

Blue	Green	Skyblue	Brown	Red	Black	Yellow	Orange	Indigo	Grey	Purple
RARS1	USE1		MEGF6	PANK3	SMG6	MRPL45	ACADSB	EMC6	IFT22	SOS2
MIR3147HG	MRPL37		PDCD6IP	BRIX1	ADSS1	GNAI2	TOGARAM1	DCTPP1	ADCK2	MYO5B
MED8	TIMM9		NRCAM	RBM17	KLF9	OST4	PDE4D	BOD1	ZNF561-AS1	PREX1
NOP9	PHB2		MGST3	CRLF3	RECQL4	RAB1B	RAB9A	ME1	CREBL2	EVI5L
RTF2	STIP1		NPTXR	WDR75	H2AC13	LINC01123	SBF2	TMEM165	PKP2	RPH3AL
F2RL3	PPAT		MAP7	NAA50	GLTP	KDELR3	RRAD	VDAC2	SNX24	CA11
PHF5A	APEX1		MTPN	CYB5R2	ARID3A	CYBA	MED13L	DOHH	MAP10	MCMBP
POMGNT2	MIB2		ABL1	IFIT5	LHPP	MRPS31	CHST7	GBA2	MYL12B	FBF1
DANCR	RBL1		HLCS	CNOT9	HAS3	ANG	POMK	HLA-DMA	MESP2	RPUSD3
FAU	CORO1C		EDIL3	STK38L	INF2	MAMDC2	POGZ	MRPS35	MFSD13A	CEP164
RCE1	DEK		GARS1-DT	USP15	MMP17	SPON2	KCNA3	KCNAB2	SERPINE1	ZP3
TMEM218	SSR3		BOLA1	IGFBP4	REEP6	RPLP0	PRRC2A	QRSL1	MMP15	FUCA2
ZNF90	RELT		MGAT5B	PDE4B	MOK	SNAI3	ORC2	KTI12	TPRN	HMG20B
TAF12	ARL3		NGB	UTP20	THBS3		HOMER1	ZNF716	ITGB5	NIBAN2
RAB30-DT	MED19		MAGEA10	BTG1	NDNF		MAP3K4-AS1	CAPN2	NPDC1	ANKRA2
PYGB	PARP9		MYO1C	MCL1	LINC01881		SIN3B	NLE1	SCARB1	LSP1
CLP1	RPS20		DCLRE1A	LYRM7	CFAP73		MYO1B	MYD88	TST	WDSUB1
ASMTL	TNFRSF8		TMEM250	UTP25	TMSB4Y		ATF4	RIOK2	ZNF362	BBS10
MGLL	COPZ1		PLPPR2	IFIT2	SLC9A3R2		CCDC174	ZNF589	ARPC4	PIERCE1
SEC61G	SAMD10		FOXO4	BMS1	ST6GALNAC6		DBR1	ERAP2	BAZ2B-AS1	ITM2C
LMAN1	IDH3B		SPINT1-AS1	NRROS	CC2D1A			GAL	CBX4	FAM53B
SOCS2	MRPS18A		ATP2B4	MYB	TRIM68			ATP10A	TMEM242	TIMP1
GMPPB	PINK1-AS		CIC	GBP1	GUCY1B1			COL27A1	TOB1	FZR1
TIMM8B	DNAJC1		SLAIN1	GTF2I	IFT88			LINC01229	PMM1	XYLT2
FKBP11	ANXA2R-OT1		LBH	ATAD1	MLXIP			CALHM6	SOX8	H2AZ2
POLR2K	GPR89A		DCAF6	HELB	NPW			PML	IFT43	SNTA1
ICMT	HLA-C		KIF26A	RAB3IP	FUNDC1			RBMY3AP	HDAC5	FLYWCH1
EIF3G	THAP12		SLC4A11	PIP4K2A	COCH			TMX1	SRD5A3	UBTD1
PROB1	MFSD3		ZNF768	PHACTR1	TCEA3			AATF	NSMCE3	TEX19
DTX4	SHISA5		MAGI3	NUCDC1	PPP1R26-AS1			DNAJC11	NANOS3	MEGF8
MUS81	CCDC9		TAF9B	FAM13A	FCGBP			EYA3	TRAPPC9	EPHX1
ARHGDI	B2M		PTPRF	BYSL	CBX7			MRTO4	MARCHF9	KLF13
ZNRD2	TYMSOS		TCIRG1	TNFSF10	ARVCF			LRP8	PPT2	NCK1
WIP11	ACOT8		C4orf50	GMEB1	TMEM54			MYBBP1A	JAGN1	STK33
PFDN1	NOPCHAP1		CADM1	DDX21	CPNE2			BNIP1	KIFC3	GIHCG
ACY3	CDC42EP5		NBR1	RFFL	CHTF18			GNL2	HMCES	RPGRIP1L
SRP19	PGAM1		LMLN	URB2	TNFRSF12A			FLI1	SPIN4	ASB2
CLPTM1L	PDIA2		RNF183	USP3	FIBCD1			UBE2D3	SLC2A8	SLC38A7

Blue	Green	Skyblue	Brown	Red	Black	Yellow	Orange	Indigo	Grey	Purple
TEKT4P2	PA2G4		BUB3	PRKCD	H4C12		ARL6IP5	PIGS	GGCT	
PTPN23	RAD54L		TBC1D5	TRIM25	ADAMTSL5		SP140L	TMEM53	H3C10	
MILR1	DOCK2		PLXNA3	MITD1	NMU		CCDC47	TPMT	KAZALD1	
ABCG1	NIPAL3		LDHD	NFKBIE	MRM2		OGFR	LASP1	DYNC1LI1	
MZB1	APBB2		CARD11	NABP1	PACS2		NOL6		PTPN4	
SCD	IFI44L		SRPK2	MOB3C	LINC02595		EIF2S1		LGALS9C	
LYPLA2	EXOSC4		H2BC20P	PAK1IP1	FBXL22		ABCF2		METTL27	
RAD9A	LAPTM5		YPEL2	TEX261	KCNH2		ZNF124		RTL8C	
DPYD	RHOA		PNPLA8	THOC1	CD3E		HSH2D		FABP1	
ZNF826P	MAP3K5		C1orf56	PATL1	RABL6		ZNF35		CGN	
GANAB	FAM86B2		ZYG11B	AMER1	ZNF571-AS1		CCDC71		DOCK9	
LMAN2	NMI		ZFP90	NOL9	SLC44A2		ALAS1		CETN2	
RAP1A	SSR2		DSCAM	MTMR4	SAPCD2		NMNAT1		ALS2	
RPL29	TMEM175		PRKACA	MIR3142HG	RIMS3		STX12		REXO5	
NBEAP1	SLC38A5		MSX1	ZNF330	SMARCD3		PRKAG2		CBFA2T2	
CMTM3	FADS3		KC6	MYC	SH3BP1		FAM98A		IRF2BPL	
FDPS	NUDT5		DCPS	DDX58	RASSF4		EIF3J		KIF1B	
PABPC4	LIPE		ITGB1	SLC11A2	DDIT3		MFAP3		TATDN2	
HNRPNU2	GCSH		B4GALNT1	MLLT1	TFEB		RNF31		PFKL	
NOC4L	CADPS2		TTC30A	IFNB1	RAB33B-AS1		ANKHD1		BIK	
RNF144A	CAV1		TCAF1	ZBTB17	BEND6		CHUK		DARS2	
PUSL1	TPRKB		TAX1BP1	EIF4A1	ZNF75A		ACO2		FMNL1	
SKP1	CELF2		SGSM2	ZNF346	MSANTD3		TXNIP		VGLL4	
SPATA24	MESD		DVL3	TNFRSF10B	INTS1		ZNF622		EPCAM	
PGM1	ATG3		ZNF862	LYRM4	LAT2		NIP7		WDR19	
NHP2	TRPT1		OGA	RRP7A	TSSK6		TP53RK		PBXIP1	
SMIM4	IFFO2		DSTYK	MAK16	TWSG1		TAF7		CRYBB1	
LINC01138	GPATCH11		TRIM59	NFKBIB	CNN3-DT		CLPB		BEGAIN	
PITHD1	EHD1		ADD3	PRAG1	GNRHR2		RBM27		FGD3	
LZIC	ZNF740		SNX16	ZHX2	RASA2		MIER2		WNT7B	
MHENCR	CAAP1		PRICKLE3	G0S2	AASDH		RAB22A		NF2	
OTUB1	SNHG19		ODF2	ZNF195	COX18		NDUFA9		WASHC5	
FGD5	BEND4		NLRP5	MGRN1	ZFTA		SEC24C		NAIF1	
BTF3L4	GRPEL2		ATG2A	BAIAP2L1	WARS2-AS1		RINT1		HSPB8	
SRM	SMARCC1		ARHGAP42	QTRT2	MTA1-DT		ENTPD1		SCAPER	
NDFIP1	KCNAB1		CLBA1	NR4A3	CTSB		SPTLC1		UBL3	
TM2D3	LINC01128		ALPK1	CCNL2	C5orf34		STKLD1		SLC1A5	
MACO1	VAMP8		ATP6V0E2	SNRNP27	LYSMD1		SF1		AMPD2	

Blue	Green	Skyblue	Brown	Red	Black	Yellow	Orange	Indigo	Grey	Purple
SF3B2	RPL36AL		TGFB3	ZDHHC21	ITPKC		LINC00519		S100A3	
CR2	SNX5		KHDRBS3	CILK1	BBS4		SLC25A28		BRK1	
CCNG1	KCNK6		ERI2	AGPAT5	FMNL1-DT		HSPA8		FLNA	
RAB26	UBE2V1		NPC1	BAP1	SH3PXD2A		PSMB8-AS1		SPINDOC	
CYB5R4	ATF1		PLEKHG2	SLC22A23	SEC61A2		C1QL3		SESN2	
RACK1	SRRT		ZEB1-AS1	PRR3	LINC02132		AASDHPP7		CCDC34	
TEX14	LTO1		TPPP	FASTKD5	EML6		CDC37L1-DT		UBXN2A	
DIAPH1	UFC1		MPP1	ZNF620	PLS1		DGUOK-AS1		NDUFA10	
HARS1	POLR2C		MNT	WNT5B	SIRT5		ANKHD1-EIF4EBP3		BMP1	
ENPP4	ZNF232-AS1		SPC24	GTPBP4	MAN1B1-DT		PORCN-DT		VPS52	
CNTF	TMEM161A		USP9X	PAICS	C7orf25		C9orf72		MICALL1	
ANAPC15	C1D		CRELD1	RAB12	C11orf71		PMF1-BGLAP		ZBTB11-AS1	
MYOM2	LRRC41		VSTM4	CFLAR	PTS				PIR	
TUSC2	IFFO1		KAT14	TERF2	CFAP298				FOXJ2	
RPS6	GALNT10		PRDM4	NOP2	CTTN				COBLL1	
LDLRAD3	ERP44		JARID2	EMSLR	MNX1				PXK	
FKBP2	PANK4		CDA	RGS1	ENC1					
RAC2	IFI35		HPSE	ZFP36	HMGB3					
PNP	RABEPK		FCER2	NUP62	NAGLU					
DCTN4	LINC02009		MROH6	NAV2	PLPP3					
CYP51A1	RPL27A		UROS	ASPHD2	FAM222A					
SELENOK	SELENOS		SHTN1	RTCB	LRRC3					
NCEH1	ELP6		BACE2	CAB39	PPP6R2					
KARS1	VAC14		POC1B	PLEK	RAB15					
ZSCAN16-AS1	LY6E		PPP2R5C	GLS	HBA2					
LAMTOR1	IP6K1		TRAF5	SLC44A5	MYO5C					
PSMF1	HYAL2		POMZP3	OGFOD1	BCYRN1					
CYP2J2	CHFR		GPAA1	PLD6	COG8					
SYK	ANXA6		FAM25BP	OTUD4	ASRGL1					
NUDC	SCAMP2		NBPF3	UBAP2L	NDRG4					
CD99	PDIA3		KRT83	PARP14						
TPBG	CRLF2		PSORS1C1	SINHCAF						
CHRAC1	MLX		LCLAT1	RRP7BP						
CEACAM21	DMAP1		ERCC6L	GNL3						
DHX34	PPP1R11		KRT6B	ADAP1						
ARPC5	DNTTIP1		GBE1	EI24						
ZNF436-AS1	TRIM27		NGLY1	SLC16A1						
RSU1	MAPK9		SEMA4D	ICE1						

Blue	Green	Skyblue	Brown	Red	Black	Yellow	Orange	Indigo	Grey	Purple
CTNNBL1	FJX1		DTX1	TMEM39A						
DNAH14	RPL21		PPP1R18	PLCL2						
TMED9	HERC6		TMEM237	PFDN2						
MRPS12	GPR89B		UBALD2	EMSY						
SPRED1	IL17RB		FAM126A	GABPB1						
MLEC	FAM241A		SNTB2	POLR1B						
ALDH1L2	SHROOM3		ACACB	PANK2						
XK	NOP58		STXBP5	RRP12						
AAR2	EEF1B2		EIF3J-DT	RNF19A						
EIF3I	DUS1L		ZDHHC20	UTP15						
SEC61A1	MGST1		EIF4E3	DCAF13						
GLT8D1	SNRPD1		SMAP1	PRMT1						
GASK1A	RPP30		CPPED1	PTPN2						
MPHOSPH6	PSMB10		H2AC6	DGKE						
TCAIM	RTRAF		SELENOW	TCF4						
PSME1	ARSA	LINC00052	PPARGC1B							
UTP4	PDIA5		MAST3	RFX5						
TM9SF3	KPNA1		ANLN	OASL						
PNO1	NRDC		ENDOV	SH2D4A						
ARHGDIA	IRF7		PEX11A	DIP2B						
TMED5	NDC1		ARHGEF9	NFKBID						
MPDU1	RNF125		AGGF1	SNX11						
ITGB7	ITGAL		TBC1D14	MTF1						
NUCD2	UROD	LINC01278	ING3							
FTSJ3	MRS2		SMARCC2	MAML1						
VKORC1L1	UBLCP1		TNRC6B	TRIM21						
CGREF1	RPL37		PALD1	KLHL18						
TRAM1	CDK11B		TMEM178B	FARS2						
SMIM12	RRS1		DLGAP4	RASA1						
RRP9	STEAP3		TRAPPC13	PGAM5						
STOML2	OPN3		PLXNA2	PPP2R1B						
ORMDL1	DENND2D		NIPA1	GMFB						
SNIP1	TAPBPL		TTC28-AS1	ANKRD40						
VCP	PSMA5		FGFRL1	DTX3L						
TUT1	SLC35E1		ZNF829	MAP4						
MTFP1	CCDC138		MAPK13	PSME3						
EMC7	RBCK1		PPM1B	TNIP2						
CASP1	CNOT8		WASF1	PDSS1						

Blue	Green	Skyblue	Brown	Red	Black	Yellow	Orange	Indigo	Grey	Purple
MTG2	PISD		HNRNPLL	ZNFX1						
PRPF19	ZW10		ITPKB	TRIM26						
NT5DC2	GLCE		SEMA4B	HOOK1						
SLC35F4	MVD		CDCA7L	RPRD1B						
TPK1	EIF3K		NUF2	IFI16						
ERI3	BCS1L		SNHG20	NCL						
ATPAF1	RBFOX2		DHRS2	MRTFA						
HSBP1	RCHY1		REPS2	ZNF506						
FEN1	BHLHA15		TMEM106B	TIFA						
TMED7	DYNLT3		PXN	IFIH1						
ATP1A3	SNORD3B-1		ARL6IP1	KCTD12						
NANP	AK3		RNF13	SMOX						
EIF3M	CDC42		ABCA2	IMP4						
CRNL1	THTPA		BUB1	CCND2						
MON1A	CAMKK2		GLIS2	RPUSD4						
SPCS3	NDUFS6		H2BC8	RAB24						
KIF9	HSPE1		ETV5	SPATA2						
EIF1AD	SPRYD3		PPP2R5A	RND1						
MKNK1	LMNB1		STRBP	ZNF430						
ANO10	NDUFB3		TMEM63C	WAKMAR2						
SHISA4	IRF1-AS1		ADCY6	ARPP19						
PDIA6	UQCRH		STXBP1	DSE						
CNTNAP3	CUTC		COA1	GBP3						
FCHSD1	RTN2		PKNOX1	IPO7						
DCAKD	RPL38		POMT1	SLCO5A1						
INTS4	DRAP1			SMG5						
SULT1A1	NSUN5			RIOK1						
SPRY4	ZDHHC3			NUP153-AS1						
CCNC	INTS11			STX11						
PEX14	SMYD5			EIF4G2						
GNG5	CCDC187			ELOVL7						
TAF9	SNRNP70			ZNF670						
WDR74	C5orf15			SGTB						
NACA	POLD4			NR1D2						
EMC8	CAMLG			NXF1						
TRIT1	TIGD2			MAFF						
PAQR7	MAN2A1			SNHG1						
SRA1	RAE1			CRIM1						

Blue	Green	Skyblue	Brown	Red	Black	Yellow	Orange	Indigo	Grey	Purple
ZNF682	GSTO1			TAP1						
MTUS1	QDPR			GRAMD2B						
PSMA3	UBE2N			FANCL						
AHCY	EMB			TMA16						
EXO5	SDHAF2			EML4						
EVI2A	MRPL4			HNRNPK						
POLR1H	CSTF3			DENR						
RMDN3	RAB6A			NAA15						
PIGO	NAA80			PLAGL2						
WASF2	SLC10A7			ZNF492						
MUL1	PURA			METTL2B						
POLR3H	ALG1			CYLD						
Gstk1	FAM27B			CCL5						
SYS1	ZNF408			DHX16						
IDI1	MRPS23			SMURF1						
TRPC4AP	SIL1			ASNSD1						
SIRT2	SIRT6			MMACHC						
SF3A1	ACADM			TRAFD1						
RSAD1	BMPR2			HDAC2						
EIF2B2	MRPL24			AGFG1						
ALDH18A1	CYB5RL			HIVEP1						
RANBP6	DNAJC8			ICAM2						
LINC01358	SNHG8			IPO5						
TRIM7-AS2	NARS2			WDR12						
UBIAD1	CKS2			IMPA1						
GPATCH3	CUEDC2			SLC39A1						
SGF29	TMCO1			UBE2V2						
GTF2B	IVNS1ABP			POLR3A						
DDN-AS1	ATF5			PHLPP1						
ZNF593	ATP5IF1			YARS2						
RPS8	GON7			PCNX3						
ZFYVE9	ZNF433-AS1			NEK4						
CACNA2D3	SACS			MACC1						
CCDC163	TMEM97			RBM6						
MTMR8	PURPL			MTOR						
BIN2	SF3A2			TRIM69						
STT3A	MLLT10			MAT2A						
MAPRE1	PSMA7			GPBP1						

Blue	Green	Skyblue	Brown	Red	Black	Yellow	Orange	Indigo	Grey	Purple
KRT10-AS1	DCTN3			CLUHP3						
TXNL1	FABP5			CSNK1A1						
SLC22A5	ODC1			TOMM70						
PHYKPL	ACACA			TMEM120B						
EMC1-AS1	SAR1A			CPEB3						
DNAJC3	AKAP8L			PEAK1						
FXYD5	PLA2G4A			MCTP1						
CISD2	TMEM126A			BNIP2						
C5orf63	GNB1L			NOC3L						
HLA-DOB	SMARCD1			SLC9A8						
ASAH2B	TCP1			RNF19B						
IFITM2	MRPL14			CDK17						
C5orf24	MT1X			CSF2RB						
PNOC	CALU			SPTY2D1						
LINC01531	RGS19			CCDC59						
SF3B5	CYP20A1			SRRM1						
ERO1B	ARF1			SFMBT2						
C11orf98				ST8SIA4						
HM13				CCDC66						
NETO1-DT				TVP23B						
GAREM1				ENTPD1-AS1						
M6PR				PBRM1						
EIF6				FAM210A						
UCHL3				TANK						
CDH18				NAGK						
TBL2				EML2-AS1						
SMIM27				SDC4						
SLC2A1				CSGALNACT1						
NRBP2				LACTB						
CHI3L2				PLEKHM2						
SLC8A1-AS1				XRN2						
TMEM80				MRPS11						
ERCC6L2-AS1				IGHMBP2						
EMBP1				THUMPD2						
EEF1A1				SLC2A6						
CSTF1				NLRP7						
PIGL				COPS2						
ALOX5AP				SDAD1						

Blue	Green	Skyblue	Brown	Red	Black	Yellow	Orange	Indigo	Grey	Purple
MIR4500HG				TIMM23						
BATF3				LPIN1						
ZNF341				EDC4						
				KLF5						
				PTP4A1						
				E2F3						
				UMPS						
				RNGTT						
				NOCT						
				ELL						
				ITPRID2						
				STEAP1B						
				THADA						
				ZNF268						
				HEATR1						
				SLC7A6						
				ATP2A2						
				GRINA						
				HLA-DRA						
				TOM1L1						
				AEN						
				MITF						
				ZNF669						
				MIS12						
				NOB1						
				NOP56						
				PPM1F						
				KCMF1						
				RPS6KC1						
				RRP15						
				SETD2						
				PROX1						
				LSM12						
				SAMD9L						
				ZFYVE27						
				PEA15						
				TDG						
				SUPV3L1						

Blue	Green	Skyblue	Brown	Red	Black	Yellow	Orange	Indigo	Grey	Purple
				IPPK						
				NOTCH2						
				RBM39						
				NOLC1						

Supplemental Table 3. GSEA using KEGG pathways of the differentially expressed genes between control and STAT1 KO MM cells stimulated with HAPLN1 matrikine.

Term	Pathway Genes	Overlap	raw p	adjusted p	Score
CYTOKINE_CYTOKINE_RECECTOR_INTERACTION	106	29	4.5648E-15	7.8058E-13	12.1411937
TOLL_LIKE_RECECTOR_SIGNALING_PATHWAY	71	18	2.8936E-09	2.474E-07	6.66106492
RIG_I_LIKE_RECECTOR_SIGNALING_PATHWAY	52	13	5.5596E-07	2.3767E-05	4.69944011
CYTOSOLIC_DNA_SENSING_PATHWAY	36	11	4.5994E-07	2.6217E-05	4.68053052
CHEMOKINE_SIGNALING_PATHWAY	118	19	2.3072E-06	7.8905E-05	4.14671407
JAK_STAT_SIGNALING_PATHWAY	82	14	2.4955E-05	0.00071121	3.21022545
NOD_LIKE_RECECTOR_SIGNALING_PATHWAY	46	10	4.2673E-05	0.00104244	3.07657261
INTESTINAL_IMMUNE_NETWORK_FOR_IGA_PRODUCTION	19	6	0.00016821	0.00359558	2.6316797
SMALL_CELL_LUNG_CANCER	64	11	0.00017205	0.00326898	2.56435872
ALLOGRAFT_REJECTION	16	5	0.00063794	0.009917	2.22524833
APOPTOSIS	71	11	0.00044007	0.00752525	2.20036175
SYSTEMIC_LUPUS_ERYTHEMATOSUS	17	5	0.00086909	0.01238452	2.12191889
LEISHMANIA_INFECTION	44	8	0.00089543	0.01177834	2.03828143
HEMATOPOIETIC_CELL_LINEAGE	36	7	0.0012374	0.01410632	1.97647153
ADIPOCYTOKINE_SIGNALING_PATHWAY	46	8	0.00121395	0.01482748	1.93607636
VIRAL_MYOCARDITIS	38	7	0.00172471	0.01638476	1.90539386
P53_SIGNALING_PATHWAY	59	9	0.00160886	0.01618322	1.87867419
NATURAL_KILLER_CELL_MEDIATED_CYTOTOXICITY	70	10	0.0015093	0.01613064	1.87031887
AUTOIMMUNE_THYROID_DISEASE	15	4	0.00434874	0.03913866	1.65481458
PATHWAYS_IN_CANCER	220	20	0.00528655	0.04519997	1.38127202
TYPE_II_DIABETES_MELLITUS	27	5	0.00769	0.06261854	1.37563393
PRIMARY_IMMUNODEFICIENCY	19	4	0.01063853	0.07909513	1.32482362
B_CELL_RECECTOR_SIGNALING_PATHWAY	62	8	0.00816474	0.06346227	1.29082058
CHRONIC_MYELOID_LEUKEMIA	65	8	0.01078747	0.07686071	1.204873
CELL_ADHESION_MOLECULES_CAMS	68	8	0.01398645	0.09566734	1.10855068
ACUTE_MYELOID_LEUKEMIA	47	6	0.02190413	0.13872619	0.98083187
TYPE_I_DIABETES_MELLITUS	16	3	0.03659446	0.19555165	0.97674503
NOTCH_SIGNALING_PATHWAY	37	5	0.02830947	0.16692828	0.92630213
GLYCOSAMINOGLYCAN BIOSYNTHESIS CHONDROITIN_SULFATE	18	3	0.04977049	0.23640985	0.87421199
NEUROTROPHIN_SIGNALING_PATHWAY	100	10	0.02686156	0.16404738	0.86246399
EPIHELIAL_CELL_SIGNALING_IN_Helicobacter_pylori_INFECTION	53	6	0.0370699	0.19208946	0.82850686
T_CELL_RECECTOR_SIGNALING_PATHWAY	79	8	0.03165908	0.18045676	0.82723984
MELANOMA	42	5	0.04571426	0.22334681	0.78594642
PROSTATE_CANCER	69	7	0.04260001	0.21425298	0.7611339

Supplemental References

1. De Bakshi D, Chen Y-C, Wuerzberger-Davis SM, et al. Ectopic CH60 mediates HAPLN1-induced cell survival signaling in multiple myeloma. *Life Science Alliance*. 2023;6(3):e202201636.
2. Huynh M, Pak C, Markovina S, et al. Hyaluronan and proteoglycan link protein 1 (HAPLN1) activates bortezomib-resistant NF- κ B activity and increases drug resistance in multiple myeloma. *Journal of Biological Chemistry*. 2018;293(7):2452-2465.
3. Jung O, Trapp-Stamborski V, Purushothaman A, et al. Heparanase-induced shedding of syndecan-1/CD138 in myeloma and endothelial cells activates VEGFR2 and an invasive phenotype: prevention by novel synstatins. *Oncogenesis*. 2016;5(2):e202-e202.
4. Zengel P, Nguyen-Hoang A, Schildhammer C, Zantl R, Kahl V, Horn E. μ -Slide Chemotaxis: a new chamber for long-term chemotaxis studies. *BMC cell biology*. 2011;12(1):21-14.
5. Tomasova L, Guttenberg Z, Hoffmann B, Merkel R. Advanced 2D/3D cell migration assay for faster evaluation of chemotaxis of slow-moving cells. *PloS one*. 2019;14(7):e0219708.
6. Markovina S, Callander NS, O'Connor SL, et al. Bortezomib-resistant nuclear factor-kappaB activity in multiple myeloma cells. *Molecular cancer research : MCR*. 2008;6(8):1356-1364.

7. O'Connor S, Shumway SD, Amanna IJ, Hayes CE, Miyamoto S. Regulation of constitutive p50/c-Rel activity via proteasome inhibitor-resistant IkappaBalpha degradation in B cells. *Mol Cell Biol*. 2004;24(11):4895-4908.
8. Runnels JM, Carlson AL, Pitsillides C, et al. Optical techniques for tracking multiple myeloma engraftment, growth, and response to therapy. *Journal of biomedical optics*. 2011;16(1):011006.
9. Chen Z, Orlowski RZ, Wang M, Kwak L, McCarty N. Osteoblastic niche supports the growth of quiescent multiple myeloma cells. *Blood*. 2014;123(14):2204-2208.
10. Lwin ST, Edwards CM, Silbermann R. Preclinical animal models of multiple myeloma. *BoneKEy reports*. 2016;5:772.
11. Campeau E, Ruhl VE, Rodier F, et al. A versatile viral system for expression and depletion of proteins in mammalian cells. *PLoS one*. 2009;4(8):e6529.
12. Caeser R, Di Re M, Krupka JA, et al. Genetic modification of primary human B cells to model high-grade lymphoma. *Nat Commun*. 2019;10(1):4543.
13. Huynh M, Chang HY, Lisiero DN, et al. HAPLN1 confers multiple myeloma cell resistance to several classes of therapeutic drugs. *PLoS One*. 2022;17(12):e0274704.
14. Roopra A. MAGIC: A tool for predicting transcription factors and cofactors driving gene sets using ENCODE data. *PLoS computational biology*. 2020;16(4):e1007800.
15. Love MI, Huber W, Anders S. Moderated estimation of fold change and dispersion for RNA-seq data with DESeq2. *Genome Biol*. 2014;15(12):550.
16. Traag VA, Waltman L, van Eck NJ. From Louvain to Leiden: guaranteeing well-connected communities. *Sci Rep*. 2019;9(1):5233.

17. Blondel VD, Guillaume J-L, Lambiotte R, Lefebvre E. Fast unfolding of communities in large networks. *Journal of Statistical Mechanics: Theory and Experiment*. 2008;2008(10):P10008.